ESS REPORT

THIRD QUARTER
APRIL 1963

ELECTROLYTIC NIOBIUM AND NIOBIUM ALLOY CAPACITORS

KEMET DEPARTMENT
LINDE COMPANY

DIVISION OF UNION CARBIDE CORPORATION

RESEARCH AND DEVELOPMENT WORK ON ELECTROLYTIC NIOBIUM AND NIOBIUM ALLOY CAPACITORS OF WET AND SOLID TYPES

BUREAU OF SHIPS CONTRACT NObsr-87478

THIRD QUARTERLY PROGRESS REPORT

JANUARY 1, 1963 - MARCH 31, 1963

ELECTROLYTIC NIOBIUM AND NIOBIUM ALLOY CAPACITORS

OF WET AND SOLID TYPES

BUREAU OF SHIPS CODE 691A2

SUBJECT:

Bureau of Ships Contract NObsr-87478
Quarterly Research and Development Report, January 1, 1963 - March 31, 1963

REFERENCE

Project Serial No. SR-0080302 ST 9600

PROGRAM OBJECTIVES

The development of 35, 50 and 100 volt niobium electrolytic capacitors of highest possible capacitance values, capable of full voltage operation at 85°C and with design objectives as listed in Military Specification MIL-C-26655 for:

(1) electrical parameters,
(2) environmental characteristics,
(3) spatial configuration and dimensions,
(4) operating temperature range (-65°C to +85°C)

Report written by:

F. E. Cariou
Project Leader, Niobium R & D
Development Laboratory
Kemet Department, Linde Company
Division of Union Carbide Corporation
Cleveland, Ohio

FOREWORD

This third quarterly report marks the midpoint of the research and development program. Up until now, the main effort has been directed to studies of various physical, chemical and electrical processing variables for capacitor anodes and foil. This work was of necessity conducted on relatively small batches of material because of the large number of parameters involved. However, it is now believed that enough information has been accumulated to outline a tentative standard processing specification for niobium sintered plugs - this specification is of course, subject to some future modifications as more information is gained in various areas. In the future, emphasis will be placed on production of larger batches of capacitors, to enable more reliable statistical data to be obtained during failure rate testing under various environmental conditions.

SUMMARY OF PROGRESS

TASK A - Work on Niobium and Niobium Alloy Sintered Anode Capacitors of Solid and Wet Types

Activity 1 - Exhaustive Trace Impurity Analysis of Niobium Materials Made by Three Different Processes (Union Carbide Metals Company)

Material 1 - niobium granules made by hydrogen reduction of pentachlorides

Material 2 - niobium granules made by carbothermic reduction of pentoxides

Material 3 - niobium slabs made by a proprietary process

A. Objective

It is expected that a co-ordinated analytical and electrical evaluation of these materials will help to identify the impurities mainly responsible for degradation of dielectric Nb_2O_5 films and thus serve as a guide for the subsequent purification studies of Activity 6.

B. Status

1. Analysis of Powders

Approximately five pounds each of materials 1, 2, and 3 have been reduced to hydrided metal powder and the analyses, as summarized in Table 1, are now complete. In some cases, analyses of the original material were approximate, since suitably sensitive methods had not yet been developed at the time of evaluation. Thus, for example, aluminium in materials 2 and 3 has not been determined with the greater sensitivity (<10 ppm) of a modified emission spectrographic technique; this will be done in the next quarter.

Considerable difficulty was encountered in the preparation of powder from material 1. However, by modification of the hydrogenation procedure, it was possible to overcome the grinding problem. Although at the 0.6 weight % level of hydrogen, the material could not be reduced to powder, it was found that a combination of cold working and retreatment in hydrogen raised the hydrogen level to 0.9%, at which point the metal could be ground successfully. Unfortunately, the level of certain metallic impurities (Mo, Cr, Fe and W) in the powder sample was also raised during this process; and, as indicated by the results of Table 1, leaching in hydrochloric acid did not completely eliminate the contaminants. A second five pound batch of material 1 will be size-reduced at Kemet during the next quarter in an effort to avoid such contamination.

2. Analytical Methods Development

As mentioned in the last quarterly report, it has been found necessary to develop special analytical methods for determination of certain elements at the low concentrations found in the three materials under study, since existing techniques are relatively insensitive. A brief outline of the principle of the method for accurate quantitative detection of some of these impurities is given below. In most cases, the same improved procedure can also be applied to tantalum analyses.

Zirconium (Sensitivity <1 ppm)

The sample is dissolved in a mixture of hydrofluoric acid and nitric acids. After removal of the nitric acid by volatilization, the solution of the sample is adjusted to contain 10% HF and 50% HCl, and then passed through an ion exchange column containing Dowex 1 anion resin. Zirconium is then determined in the eluate either by spectrophotometry with phenylfluorone or by emission spectroscopy. The separations for this element were checked quantitatively by use of radioisotope Zr^{95}.

Titanium (Sensitivity (<1 ppm)

After the same dissolution and ion exchange separation employed for zirconium in niobium, the titanium is determined in the eluate by a spectrophotometric method, which involves extraction of the titanium thiocyanate complex with tri-n-octylphosphine oxide (TOPO) dissolved in cyclohexane. Alternatively, an emission spectrographic method can be used.

Vanadium (Sensitivity (<1 ppm)

Vanadium content is determined emission spectrographically along with titanium and zirconium, after removal of the niobium in the ion exchange column.

Tin (Sensitivity 10 ppm)

Spectrophotometric method: After dissolution of the metal in a mixture of HF and HNO_3, the fluoride and nitrate are removed by fuming with H_2SO_4. The solution is so adjusted that the acidity corresponds to 1M HCl and 2M H_2SO_4. The tin is then extracted with 0.01M tris (2-ethylhexyl) phosphine oxide (TEHPO) in cyclohexane. The colour is developed with pyrocatechol violet.

Emission Spectrographic method: The tin content can also be determined emission spectrographically along with Ti, Zr and V, after ion exchange separation of niobium and tantalum.

Aluminium (Sensitivity <10 ppm)

The niobium metal is converted to oxide by ignition, mixed with graphite and analyzed emission spectrographically using an AC arc double cap mix technique.

Silicon (Sensitivity 5 ppm)

The niobium metal is converted to oxide by ignition, mixed with graphite and germanium oxide (internal standard) and analyzed emission spectrographically using a DC arc.

Lithium (Sensitivity 10 ppm)

After acid dissolution of the metal sample, the acid is removed and the sample converted to niobium oxide. The oxide is then mixed with graphite and the lithium content determined emission spectrographically.

Activity 2 - Preparation of Niobium-Tantalum Alloys

A. Objective

Union Carbide Metals Company is to make five pound batches of five different alloy compositions (0, 25, 50, 75 and 100% niobium by weight) and convert them into capacitor grade powder. The alloys are to be analyzed for interstitial impurities as well as for homogeneity; and several pounds of each material are to be submitted to Kemet for evaluation.

B. Status

The experimental work has been completed and approximately five pounds each of four alloys have been shipped to Kemet in the form of hydrided -200 mesh powder. The fifth "alloy" (100% Nb), Material 2 of Activity 1, has been on hand at Kemet since the first quarter.

Analysis of the -200 mesh powders, together with the quantity recovered and shipped, are listed in Table 2. The increase in tantalum over the nominal composition was caused partly by tantalum pickup from the tantalum-lined ball mill.

In view of the relatively high nitrogen contents of the alloy powders, it is intended to prepare an additional five pound lot of the 50% Nb-50% Ta alloy with a lower nitrogen level. For this purpose, 7½ pound lots of hydrided niobium and tantalum roundels have been ball milled in argon to -200 mesh powder. The lot analyses for these materials are given in Table 3.

After dehydriding, a five pound ingot will be prepared by blending, compacting, sintering and cold-rolling. The alloy will then be hydrided at Union Carbide Stellite Company in a special furnace designed to minimize the danger of contamination.

Activity 3 - Determination of Optimum Conditions for Removal of Carbon from Niobium

A. Objective

The object of this study at Kemet is to determine the efficacy of high temperature vacuum prepurification and oxygen predoping of niobium materials, in reducing the level of carbon in sintered anodes, thereby improving their electrical performance.

B. Status

The program as outlined in the flow diagram of Figure 1 has now been completed. The results of the purity analysis and electrical wet testing of sintered anodes were described in the Second Quarterly Report (Table 5, Page 24). On the basis of the information available at the time, it was apparent that:

(1) vacuum prefurnacing and oxygen doping are not necessary to reduce the carbon level in plugs from as high as 550 ppm down to about 20 ppm, provided that the plugs are vacuum sintered at 2100°C for 30 minutes after pressing.

(2) fairly wide variations in C, O, N and Fe levels had no pronounced effect on breakdown voltages on wet test.

Since then, small batches of 10 plugs each, from the groups represented by analyses C(10), C(11), C(12), C(13), C(14) and C(15) of Figure 1, have been processed through to canning and subjected to tests of leakage current, capacitance and dissipation factor at 35 volts D.C. bias.

The processing details are listed in Table 4 and the results of the initial evaluation are presented in Tables 5A and 5B. From the tabulated electrical measurements and yield figures, it appears that the control powders, which received no special treatment prior to pressing into plugs, yielded the best anodes. As indicated in Table 5B, almost all capacitors survived 120 hours ageing at 35°C and 38 volts; however, when they were then put on life test at 85°C, 35 volts, 77 of 83 units failed within 500 hours. Unfortunately, the populations of individual sub-batches were too small to provide reliable statistical failure rate data. Of the seven capacitors surviving 500 hours life testing, five are from sub-batch C(15) of lot BM 812 material. Comparison of the analytical results for this sub-batch with that of several other sub-batches (Table 5 of Second Quarterly Report) does not reveal any significant difference in purity.

Larger groups of plugs from sub-batches C(13), C(14) and C(15) of material BM 812 and C(10) and C(15) of material 2121, have been similarly processed into solid capacitors and submitted to ageing at 35°C and life testing at 85°C. The history of these groups will be described in the next Quarterly Report, when enough failure rate data have been accumulated.

Activity 4 - Determination of Optimum Anodization Conditions for Niobium Anodes

A. Objective

The object of this work is to determine the best formation electrolyte and formation conditions (formation temperature, current density and time) for niobium anodes.

B. Status

In the last quarterly report, the best known formation conditions, determined on the basis of wet test measurements of breakdown voltage and leakage currents, were summarized. Other studies are being carried out, as time permits, to further optimize the formation procedure.

Figure 2 illustrates the effect of electrolyte conductivity on the breakdown voltage of niobium anodes on wet test at 25°C and a current density of 50 ma/gm of material. In all, a total of nine conductivity modifications of proprietary electrolyte Y_1 were tested, with the results shown. Clearly, a conductivity in the range 3 to 4 x 10^{-4} $(ohm\text{-}cm)^{-1}$, corresponding to an electrolyte resistivity of 2500 to 3300 ohm-cm, provides the best results.

Figure 3 illustrates the effect of electrolyte temperature on the breakdown voltage of niobium anodes on wet test in proprietary electrolyte Y_1, at a formation current density of 50 ma/gm of material.

There appears to be a continuous increase in breakdown voltage with decreasing temperature in the range between 90°C and 0°C. This suggests that measurements should be extended to sub-zero temperatures.

A program has been started to evaluate the effect of formation temperatures in the range from below 0°C to +25°C, on the electrical properties of completed units on solid test. Also under study in this same program are the use of ultrasonic agitation during formation, and the optimum formation time. The results will be described in the Fourth Quarterly Report.

Activity 5 - Determination of Optimum Processing Conditions for Solid Niobium Plug Capacitors

A. Objective

The object of this work is to determine the best processing methods for the preparation of solid niobium plug capacitors up to the canning stage. Parameters to be studied in this phase include optimum particle shape and distribution, green density of plugs, sintering conditions, chemical etching and reformation-impregnation conditions.

B. Status

(a) Sub-Activity 5.3 - Determination of Optimum Particle Size Distribution for Niobium Powders Used in Pressing Capacitor Anodes

In the Second Quarterly Report, an outline was given (Figure 4 and Tables 10, 11) of a study to determine the effect of variations in niobium powder particle size, as classified with metal sieves, upon the wet electrical properties of sintered anodes. The influence of vacuum high temperature metal prepurification, chemical cleaning of powder, and variations in anode densities, on the electrical properties, were also to be evaluated. In the following sections, a summary is given of the more interesting results to date.

Chemical Analyses

The analytical results for the "as-received material", the hydrogen contents of the eight hydrided powders, and the complete analytical results for the same powders after dehydriding, are listed in Table 6.

The efficacy of prefurnacing at 2200°C in reducing the impurity content of the niobium will be noted. The prefurnaced powders II, III and IV contain less than half the amount of carbon (30 to 60 ppm) found in the control sample (100 to 120 ppm). Similarly, a significant reduction in iron content is evident - from 40-50 ppm to 10-30 ppm. The bromine etch treatment (B powders) is apparently also effective in removing metallic impurities such as iron.

The increase in oxygen content of prefurnaced material over that of the "as-received" powder is believed to be a function of the increase in surface area during processing.

Powder Particle Sizes

The powder size distributions as determined by a Micromerograph are listed in Table 7, which indicates the weight percentage of powder in each distribution cell. The cell widths in column 1 vary as the $\sqrt{2}$ and correspond to the sequence of aperture sizes of standard Tyler screens, which are based on the Gaussian distribution generally displayed by milled powders. At the bottom of the table, each powder distribution has been characterized by a "geometric mean particle size" in microns given by:

$$G.M.S. = \sqrt[100]{x_1^{n_1} + x_2^{n_2} + - - - - - + x_i^{n_i}}$$

where x_i = the midpoint of the particle size distribution cell (in microns) and

n_i = percentage of the total material in the size interval represented by x_i.

The distributions and averages are based on the sieve sizes (100, 140, 170, 200, 230, 270, 325 and 400) used. It is of interest to note that sieve analyses and Micromerograph results do not correlate exactly; for example, all the -400 mesh powders (I and II) appear to contain some particles larger than the 400 mesh screen aperture of 37 microns. This result is probably due to the irregular, non-spherical shape of the majority of particles; thus, some ellipsoidally shaped particles may pass through the screen if their major axes are properly oriented during sieving, but would necessarily be treated by the Micromerograph as of larger screen size.

Nitric acid-water screening and bromine etching appear to be about equally effective in removing fines from -400 mesh powders, since no particles less than 4 μ in effective diameter remain in significant quantities after either treatment. However, as might be expected, since bromine attacks niobium metal, the bromine treatment apparently reduced the average particle size of the coarser materials, especially the -200/325 (III) powder.

Figures 4A and 4B depict distributions of powder as a function of particle size (logarithmic scale). Figure 4 compares the four -400 mesh powders (I and II) and shows practically the same distribution for each, with tails extending into the finer particle sizes. Figure 5 compares the four powders which were washed in nitric acid. As expected, the 200/325 mesh powder (III) has the coarsest and narrowest size distribution, while the blend (IV) distribution extends all the way from 105 microns down to 4.7 microns.

Dimensional Characteristics and Densities

See Second Quarterly Report (Table 11 and Figure 5).

Plug Pore Size Distribution

The data resulting from an investigation of pore size distributions in sintered plugs pressed from the 16 different powders, are summarized in Table 8. From the table it is clear that, for all powder distributions, the total porosity decreases markedly with increasing plug density, with the effect being greater for the finer powder sizes.

Apparent pore diameters as a percentage of total porosity are distributed normally, as indicated in Figure 6 for the blended powder. In general, the higher the sintered plug density, the smaller the pores become, down to well below 5% of total porosity, at which point all curves "tail-off", indicating a small percentage of very small-diameter pores.

Again, from Table 8, the finer powders I and II contain pores of smaller diameters (averages 3.7 to 5.7 microns) than the coarse powder III (averages 6.3 to 15 microns). The blend IV results encompass those of the other powders, with averages from 3.7 microns for dense plugs to 8.0 microns for the more porous anodes.

The last column in the table gives the effective surface area of the plugs as determined by wet test measurements of capacitance. It is intended to check these calculated areas by means of sorptometer measurements, since there is no rigorous method of calculating corresponding areas from the porosimeter measurements themselves. The results indicate that pores with diameters as small as 3 microns are "useable".

Breakdown Voltage Evaluation of Powders

The results of breakdown voltage tests of anodes pressed from the 16 different powder variations, are plotted as a function of sintered density in Figure 7. Each point on the graph represents the average for at least two plugs formed individually at 25°C in proprietary electrolyte Y_1 at a current density of 50 ma/gm. The values employed have been corrected for the voltage drop across the electrolyte. It will be noted that the net breakdown voltage increases with increasing sintered density, the extent of the dependance varying with the particle size distribution of the powder. Also, the coarsest powder (III) plugs, which contain no "fines", display higher breakdown voltages at all densities; similarly, the plugs from the blend (IV), containing a larger percentage of coarse particles, attain higher voltages than do the anodes pressed from -400 mesh powders (I and II). Finally, the prefurnaced powder (II) plugs reach somewhat higher voltages at the higher densities, than do the control powder (I) anodes - again reflecting the reduced carbon and iron contents of the prepurified material.

Figure 8 shows the breakdown voltages as a function of the geometric mean particle size (GMS) of the powder (Table 7) from which the plugs were pressed to the intermediate (Y) density.

It will be noted that the breakdown voltages increase from 320 volts for a low GMS powder to 420 for a high GMS material, and that the nitric acid-cleansed, water screened powders and the bromine-etched powders give essentially the same results.

Wet Electrical Evaluation of Powders

Table 9 summarizes, for the 16 powder variations, the results of:

(1) D.C. terminal leakage current tests in electrolyte Y_1 at 25°C at 150 and 200 volts (75% and 100% of formation voltage) after 4 hours at V_F = 200 volts.

(2) Capacitance and dissipation factor measurements in 30% H_2SO_4 at 25°C, at 120 and 1000 cps, with an applied bias voltage of 12 volts.
The capacitance measurements have been converted into equivalent charge numbers and size factors to facilitate direct comparison of results, by avoiding apparent inconsistencies caused by minor variations in plug dimensions and densities. Each electrical property characteristic represents the average of from four to seven individual measurements. Figures 9, 10 and 11 show the variation of size factor S^1, dissipation factor D.F. and terminal leakage current I_L with sintered anode density, while Figures 12, 13 and 14 indicate the variation of the same electrical parameters with geometric mean particle size of powders.

As demonstrated by Figure 9, the size factor increases with increasing percentage of fines in the powder. Although the influence of density is apparently small, there appears to be some evidence of an optimum density (maximum S^1) for each particle distribution. However, from Figure 12, it is evident that S^1 increases sharply from about 180 mC/in^3 at a GMS of 65 microns to 320 mC/in^3 at a GMS of 22 microns, suggesting that the primary key to higher size factors is the use of powders of small average particle sizes.

The dissipation factor variation with anode density displays the same behaviour for tests at 120 and 1000 cps, although magnitudes are, of course, different. Figure 10 portrays the results for 120 cps measurements, indicating that D.F. increases for the finer powders and with increasing sintered density. The density dependency is greater for the fine powders I and II. No explanation can be offered for the minimum in the curve I, for the "control sample" anodes. Figure 13 compares the dissipation at the two test frequencies as a function of geometric mean particle size. The dissipation factor at 120 cps is about 1%, virtually independent of GMS over the range of particle sizes investigated. On the other hand a more pronounced dependence will be noted at 1000 cps, with the dissipation factor ranging from about 5% for a GMS of 65 microns to 7% at a GMS of 22 microns - this may be due to a higher dissipative contribution from the dielectric oxide layer as the particle size is reduced.

Again, the particular powder cleaning technique used is shown to be relatively unimportant.

In Figure 11, the normalized terminal leakage currents per unit capacitance are plotted against sintered anode density. It will be noted that the terminal currents at the end of formation appear to be a minimum for the density range 5.25 to 5.50 gm/cc and are lowest at 200 volts, (i.e., 100% of formation voltage) for the powder blend (IV). Similarly, for tests at V_F = 200 volts, the leakage is apparently lowest for a mean particle size of 30-35 microns, as illustrated in Figure 14. Under these test conditions, the bromine etch treatment appears to lead to slightly lower leakages than the nitric acid cleaning.

Further Work

To explore in more detail the significant increase in size factor with decreasing particle size, the -400 mesh powders are being further classified with Infrasizer equipment, which operates on an air elutriation principle. While this work is well under way, the description will be deferred to the next Quarterly Report, when the results will be complete.

In addition, the powders and plugs are undergoing examination of particle and pore size distributions by adsorption (Sorptometer) and optical (Zeiss Particle Analyzer) techniques.

(b) Sub-Activity 5.5 - Determination of Optimum Impregnation and Reformation Methods

The impregnation-reformation study described in the flow diagram of Figure 6 , in the Second Quarterly Report, has been completed.

Test II.1 - Porosity Measurements for Sintered Anodes

A porosimeter test on several plugs gave an average value of 29% total porosity, with 92% of the pore diameters in a narrow range between 3 and 7 microns.

Test II.3 - Breakdown Voltage Tests of the Anodes

Maximum breakdown voltages were determined by individual formation of five anodes in electrolyte Y_1 at 25°C and a current density of 50 ma/gm. The average value obtained was 315 volts, from which the niobium material can be rated as of "good quality".

Test III.1 - Determination of MnO_2 Content of Plugs as a Function of the Number of Dips in $Mn(NO_3)_2$ and of Pyrolysis Temperature

After individual weighing and labeling, three groups of 10 plugs each were anodized to V_F = 200 volts under the standard conditions described above.

After 2 hours at V_F, the anodes were washed, dried, reweighed individually and finally impregnated and pyrolyzed as follows:

(a) Pyrolysis temperature 275°C - 2, 4, 6, 8 and 10 dips.
(b) Pyrolysis temperature 350°C - 2, 4, 6, 8 and 10 dips.
(c) Pyrolysis temperature 425°C - 2, 4, 6, 8 and 10 dips.
The impregnation and pyrolysis was carried out under standard (proprietary)conditions.

After impregnation, the anodes were dried 110°C for 30 minutes, to minimize errors introduced by moisture pickup, then individually reweighed and the total MnO_2 pickup calculated. Then, since the MnO_2 deposit of primary interest is that contained within the plug pores, the buildup on the plug exteriors was carefully scraped off with a sharp edge and the plugs reweighed again. This procedure furnished a simple determination of the MnO_2 content of the plug pores as a function of both pyrolysis temperature and of the number of dips in $Mn(NO_3)_2$ solution. All plugs were then submitted to the analytical laboratory, where the MnO_2 was leached out of the pores and a spectrophotometric determination of the total Mn contents made. From these measurements, the MnO_2 content was recalculated assuming complete stoichiometry (i.e., a Mn:O ratio of 1:2 such that all of the Mn is in a +4 oxidation state) and the data compared with the results obtained by the simple weighing method. The results are summarized in Table 10, from which it can be seen that a reasonably close correlation of results was obtained by the two methods. The analytical values are higher, suggesting that the assumption of complete oxidation of the $Mn(NO_3)_2$ solution within the pores is not quite correct; i.e., the semiconductor composition is actually MnO_{2-x} where $x \leq 0.2$. The MnO_2 deposit growth, as a function of number of impregnation dips and of pyrolysis temperature, is shown in Figure 15. It will be noted that the total MnO_2 buildup increases with higher pyrolysis temperatures; whereas the internal MnO_2 pickup is virtually independent of temperature and is either beginning to saturate after 8 to 10 dips, or else further penetration into the plug interior is blocked by external MnO_2 buildup. From these results it is concluded that little or no improvement would be realized by increasing the pyrolysis temperature above 300°C or the number of dips above 10.

Test III.2 - Determination of the Effect of Pyrolysis Temperature and Dip/Reformation Sequence on Electrical Properties of Anodes

On the basis of previous tests, including some work under Test II.3 described in the Second Quarterly Report, a formation voltage of 200 volts in electrolyte Y_1 at 25°C and 50 ma/gm formation current density were chosen as standard conditions for this study. Also, a preheat treatment in air at pyrolysis temperature, after formation but before impregnation, was singled out for further investigation, since it appeared to improve leakage currents of anodes on wet test.

Fourteen batches of capacitors, ranging in size from 5 plugs to 19 plugs each, were formed as described above for 4 hours and then washed for 1 hour in boiling demineralized water. Next, each batch of anodes, (with the exception of batch Nos. 12 and 14) was divided into sub-batches A and B, which were treated similarly, except that sub-batches A were preheated in air at the same temperature as was used subsequently for pyrolysis, whereas sub-batches B received no preheat treatment. All preheated capacitors were then reanodized for 30 minutes at 200 volts and rewashed.

The effect of pyrolysis temperatures ranging from 225°C to 425°C, upon electrical characteristics of solid capacitors was then studied. Conversion and cooling times were the same as in other studies with the exception of batches 12 and 14, for which, because of the lower conversion temperature employed, it was suspected that a longer pyrolysis time would be required to effect complete conversion of $Mn(NO_3)_2$ to MnO_2.

Capacitor batches with a total number of $Mn(NO_3)_2$ dips of eight or ten, were further sub-divided by choice of either a single reformation at 70 volts after the last dip, or a split-dip reformation sequence in which the first reformation at 70 volts after the first 4 or 5 dips was followed by an additional 4 or 5 dips and finally a second reformation at 65 volts. All reformations were carried out in 0.01% H_3PO_4 at 25°C. In an additional test, one or two anodes from each batch were reformed separately up to a maximum voltage V_{RF} max. (greater than 70 volts) at which the anode broke down or displayed an excessively high leakage current which did not decrease with time.

All anodes were carbon and silver coated and soldered in C size cans, using standard methods. Leakage currents of finished capacitors were then measured at 25°C at applied D.C. voltages of 15, 25 and 35 volts; and capacitance and dissipation factor measurements were made at 25°C and 12 volts D.C. bias, at 120 cps and, in some cases, at 1000 cps.

The results of the solid evaluation are summarized in Tables 11A and 11B, from which the following facts emerge:

(1) Pyrolysis temperatures greater than 275°C degrade the electrical performance in so far as leakage current and yields are concerned. Since the dissipation factor is almost independent of pyrolysis temperature, the higher capacitances realized at higher temperatures are probably due to small changes in the dielectric thickness rather than to more effective conversion of $Mn(NO_3)_2$ to MnO_2.

(2) Although the yields of good capacitors are highest for pyrolysis temperatures of 225°C and 250°C, no substantial improvement in the magnitude of leakage currents is achieved over batches pyrolyzed at 275°C. Moreover, at the lower temperatures there is a substantial loss of capacitance and an increase in dissipation factor, indicating incomplete conversion of $Mn(NO_3)_2$ in plug pores.

(3) A preheat treatment, followed by reanodization before impregnation, produces little or no consistent improvement in performance, and, especially at pyrolysis temperatures higher than 275°C, leads to substantially lower yields.

(4) A split-dip reformation sequence consisting of: four $Mn(NO_3)_2$ dips, first reformation, another four dips and a second reformation, produces the best capacitors.

Leakage currents measured on individual plugs are plotted against reformation voltage, for various pyrolysis temperatures, in Figure 6. As in the case of canned capacitors, a systematic deterioration of anode quality with increasing pyrolysis temperature will be noted.

Capacitors surviving the preceding tests were next aged for 400 hours at 25°C and a D.C. voltage of 37 volts. During this test, 11% of the capacitors failed catastrophically. The remaining units (78 capacitors) were put on life test at 85°C, 35 volts. As indicated by the linear plot of Figure 17, the failure rate of niobium solid capacitors on life test can be described accurately by the same Weibull distribution function as has been applied at Kemet to testing of solid tantalum capacitors. For the present niobium units, the computed instantaneous failure rate at 1000 hours amounts to about 25% per 1000 hours.

Other parameters of interest, some of which are already under investigation, include optimum reformation (chemical vs. dry) conditions, chemical impregnation of plugs with MnO_2 at lower temperatures and improved methods of carbon coating and canning.

Activity 6 - Preparation of Highly Purified Niobium Powders

A. Objective

After the three materials described under Activity 1 have been analyzed and evaluated, a process will be selected by which the important impurities can be removed. It is planned to add certain impurities deliberately in order to determine their effect upon the electrical properties of anodized films.

It is also intended to evaluate another type of high purity niobium material, in the form of microspheres of a selected particle size distribution.

B. Status

(a) Preparation of High Purity Niobium Pentoxide

Bench scale evaluation of an ion-exchange procedure for preparation of high purity Nb_2O_5 has been completed, and production of material on a larger scale has been in process for about one month.

Difficulties were experienced in attempts to make ultra high purity oxide using the "pure" niobium materials of Activity 1 as a starting material. It is necessary to dissolve the pure metal in an $HF-HNO_3$ solution, which later results in a fouling of the ion exchange columns with nitrate ions. On the other hand, it is possible to dissolve Nb_2O_5 in a pure HF solution which causes no subsequent difficulties. Consequently, a wet Nb_2O_5 cake material, resulting from liquid-liquid extraction, has been used as a starting material in recent work.

At the end of March, about one pound of ultra pure Nb_2O_5 was available for reduction to metal, while another 102 grams were ready for qualitative analysis. An additional 180 grams has been set aside for additional purification, since the titanium content was too high (about 10 ppm). Another pound of oxide in solution has been removed from the exchange column for further treatment. It is expected that a total of at least four pounds of oxide will be available early in April, 1963.

The Nb_2O_5 is generally of excellent quality, on the basis of qualitative tests for trace elements. Analysis of the first pound indicated the following impurity levels: F < 100 ppm, W 4 ppm, Ti 3 ppm, Si < 10 ppm and Ta < 100 ppm (not detectable by direct x-ray examination).

(b) Reduction of Nb_2O_5 to Nb Metal

Two trial furnace reductions were carried out to determine the required stoichiometry between the oxide and the spectroscopic purity graphite to be used in reduction to the metal. Three mixes of 30 grams each were prepared with 1.5, 3.0 and 5.0% excess Nb_2O_5. The carbon level in the resulting metal was below 45 ppm, but the oxygen level was still up around 10,000 ppm. Therefore, further adjustments of the Nb_2O_5-carbon ratio are required before reduction of large quantities of oxide can be undertaken.

The silicon and tungsten contents of the niobium metal were 10 ppm and 40 ppm respectively, indicating a pickup of about 35 ppm of tungsten during the reduction operation.

Samples of the ultra high purity niobium in the form of powder should be on hand at Kemet by the end of April.

(c) Preparation of Niobium Microspheres

Approximately two pounds of high purity niobium microspheres in the form of -200 mesh material have been prepared at the Linde Crystal Products Department. This powder will be shipped to Kemet some time in April.

Activity 7 - Determination of Optimum Anodization Conditions for Niobium Alloy Plugs

A. Objective

The object of this work is to determine the best formation electrolyte and formation conditions (formation temperature, current density and time) for niobium anodes pressed from Nb-Ta alloy powders made under Activity 2.

B. Status

Preparation of plugs from alloy powders is scheduled to begin during the next quarter. The work under Activity 4 will be used as a guide to curtail the effort expended in this activity.

Activity 8 - Determination of Optimum Processing Conditions for Niobium Alloy Plug Capacitors

A. Objective

The objectives of this work are similar to those outlined for pure niobium powders under Activity 5.

B. Status

The processing work will be started during the next quarter, using the results of Activity 5 as a guide.

Activity 9 - Determination of Optimum Fill Electrolyte for Wet Plug Capacitors

A. Objective

The object of this phase is to determine the best operating electrolyte for wet capacitors with regard to compatibility with the dielectric, range of temperature operation, and dissipation factor.

B. Status

All the necessary components and tooling equipment for platinization of silver cans, assembling finished capacitors, and affixing lead wires has been built, and satisfactory sealing techniques have been developed for corrosive electrolytes.

Difficulty has been experienced in finding a compatible fill electrolyte which provides good finished units rated at 2-3 μf and 100 volts at 85°C. Capacitors with these specifications and low dissipation factors (1%-3%), have been made, which display very low leakage currents (<0.05 μa) at 25°C after several hundred hours of ageing at 25°C. However, when these units are life tested at 85°C, 100 volts, failure occurs within a few hundred hours, due to excessive generation of gas within the cans which eventually results in blow-out of electrolyte through the seals. This is believed to be caused by etching attack on the niobium underlying the oxide at 85°C.

Other less corrosive fill electrolytes are known, which are compatible with the metal-oxide system at high temperatures; however, units made with these electrolytes have suffered from high dissipation factors.

This work will be described in more detail in the Fourth Quarterly Report, when, it is expected, the difficulties will have been overcome.

TASK B - Work on Niobium and Niobium Alloy Foil Capacitors of Wet Type

Activity 2 - Preparation of Five Different Niobium-Tantalum Alloys

A. Objective

Haynes Stellite Company is to prepare four pound lots of five different alloys of tantalum with niobium (0, 25, 50, 75 and 100% tantalum by weight) by electron beam melting of high purity materials. Two pound quantities of each alloy are to be supplied to Kemet in the form of recrystallized 0.010" thick foil, for electrical evaluation. Samples are also to be submitted for impurity and homogeneity analyses at Union Carbide Metals Company.

B. Status

The samples of all alloys in the form of 0.010" thick sheet have been received at Kemet and samples have been submitted for analysis.

Activity 3 - Preparation of Niobium-Platinum Alloy

A. Objective

A four pound lot of a Nb - 0.1 weight % Pt alloy is to be made at Haynes Stellite Company by electron beam melting of suitable pure constituent materials. A two pound quantity is to be supplied to Kemet in the form of recrystallized 0.010" thick foil for electrical evaluation. A sample is also to be submitted for impurity and homogeneity analysis at Union Carbide Metals Company.

B. Status

The samples of this alloy, for both electrical and analytical evaluation, have now been received.

Activity 4 - Determination of Optimum Processing Conditions for Niobium and Niobium Alloy Foils

A. Objective

The objective of this work is to determine the best metallurgical, chemical cleaning and anodization processes for pure niobium foil and for the various alloys described in the preceding sections.

B. Status

Several hundred 1 cm x 5 cm x 0.010" thick specimens, with 0.5 cm x 2 cm long tabs at one end, were cut from the "as-rolled" Parmec niobium sheet made under Task B, Activity 1. After 10 cm long x 0.030" diameter niobium lead wires had been welded to the tabs, the foils were subjected to a cleaning treatment consisting of:

(1) degreasing in a hot Alconox solution and then in A.R. grade acetone
(2) thorough washing in hot demineralized water
(3) etching in a solution consisting of 55% by volume of 96% H_2SO_4, 25% by volume of 70% HNO_3 and 20% by volume of 48% HF.
(4) rapid rinsing in several changes of boiling demineralized water.

After etching, the foils were stored in demineralized water in a covered polyethylene container until used in experiments.

These foil specimens were used as control material to evaluate some 31 different electrolytes, listed in Table 12. The assessment of electrolyte suitability was based on:

(1) measurements of maximum formation voltage at 25°C and 90°C, for constant current densities J of 1 ma/cm^2 and 10 ma/cm^2.
(2) measurements of terminal leakage current at 100% V_F in the formation electrolyte, followed by wet tests of leakage current, capacitance, and dissipation factor in 30% H_2SO_4 at 25°C and 120 cps with an applied D.C. bias of 75 volts.

Breakdown Voltage Measurements

In the breakdown voltage tests, up to four foil specimens were examined individually under each set of conditions (electrolyte, current density and temperature), while for the leakage current tests, three foil specimens were formed together but tested separately.

The results of breakdown voltage measurements for the electrolytes are summarized in Table 12. The group of electrolytes evaluated include all of those tested previously on porous anodes in Task A, Activity 4. The additional electrolytes were selected on three bases:

(1) Tests on electrolytes containing nitrate ions, hydroxyl ions, sulphate ions, arsenate ions and oxalate ions were considered of interest in providing more information concerning the influence of electrolyte on anodic film properties.
(2) In order to further optimize the electrolyte, conductivity modifications were needed of some of the proprietary electrolytes (Y_1, Y_2, Y_3) found to provide superior formation characteristics for both plugs and foil.

(3) The Y series of electrolytes all contain a fixed amount of a proprietary additive, the conductivity modification being achieved by variation of the acid content of the solution. It was considered of interest to change the fixed amount of additive in another series of electrolytes (the X series) covering the same conductivity range.

From Table 12, it is evident that the Y series of electrolytes provide the highest breakdown voltages, with Y_7 the best of all. It should also be noted that the maximum attainable voltages for some of the poor electrolytes are improved by use of a higher current density, whereas for the good formation electrolytes and some others, there is virtually no change of V_{BD} with current density.

The breakdown voltages for the X and Y series are plotted as a function of conductivity in Figure 18, from which it is clear that the optimum conductivity for foil formation is in the range 0.2 to 0.5 x 10^{-4} $(ohm\text{-}cm)^{-1}$, corresponding to an electrolyte resistivity of from 20,000 to 50,000 ohm-cm. This is to be compared with the optimum conductivity range of about 3 to 4 x 10^{-4} $(ohm\text{-}cm)^{-1}$ (Figure 2) for niobium anodes. The difference is probably due to the heating effects produced in the plugs when the electrolyte conductivity is too low, because of the intricate network of fine internal pores.

Table 13 summarizes the results of breakdown voltage tests at 90°C for a few of the better formation electrolytes. It is evident that, as was found previously for niobium plugs, formation of foil at elevated temperatures is undesirable, since the maximum attainable formation voltages are greatly reduced. Again, the rapid rate of film growth (dv/dt values) and the considerable improvement in attainable voltages realized by using a high formation current density of 10 ma/cm^2, should be noted.

Table 14 lists the results of another study in which foil specimens were anodized up to maximum attainable voltage in one electrolyte, then etched to dissolve the oxide layer, and finally reanodized again to breakdown in electrolyte Y_1. From the results, it appears that two different effects of electrolyte on anodic film growth are possible:

(1) In "poor" electrolytes such as nitric, acetic, and malonic acids and ammonium nitrate, a limiting thickness of oxide is reached due to some breakdown process occurring in the electrolyte itself, perhaps in the double layer.
(2) In "good" or "excellent" electrolytes such as phosphoric acid and the proprietary Y's, the limiting thickness of oxide is controlled by crystallization or breakdown in the anodic film itself due to physical or chemical defects. In this case, the difference between one electrolyte and another is in their relative abilities to suppress such film thickness limiting mechanisms.

Leakage Current, Capacitance and Dissipation Factor Measurements

Other electrical evaluation studies were restricted to three of the Y series electrolytes, which proved superior in the preceding tests. At least three foil specimens were anodized to V_F = 300 volts at a current density of 1 ma/cm^2, in each of Y_1, Y_3 and Y_7 electrolytes at a formation temperature $\leq$ 25°C. Terminal leakage currents were measured at 100% V_F after one hour at formation voltage. After rinsing, the specimens were then transferred to a 30% H_2SO_4 test solution at 25°C, and measurements were made of leakage current at 75 volts D.C., and of capacitance and dissipation at 120 cps and 75 volts D.C. bias. The results are given in Table 15, from which it is evident that Y_7 is also the best electrolyte tested from the standpoint of dissipation factor and leakage current.

Activity 5 - Determination of Optimum Fill Electrolyte for Niobium and Niobium Alloy Foil Capacitors

A. Objective

As in Task A, Activity 9, the purpose of this work is to determine the best fill electrolyte from the standpoint of chemical activity, conductivity and range of temperature operation.

B. Status

The following processing equipment has been developed:

(1) lead wire bending equipment
(2) welding equipment for attaching leads to anode and cathode foils
(3) a special formation tank for anodizing foils
(4) sealing equipment
(5) Equipment for butt-welding solderable lead wires to the niobium foil leads.

Using the satisfactory formation conditions determined under Activity 4, an investigation of different fill electrolytes for operational service between -55°C and +85°C has been started. A sealing technique for foil units has been perfected, but completed rolled assemblies are needed to properly test the seals and fill electrolytes under various environmental conditions.

The special foil winding machinery for assembling large foil capacitors is still in development. In the meantime, short lengths of hand-wound foil are being evaluated.

TASK C - Basic Studies of Tantalum and Niobium Single Crystals, Sputtered Films and Polycrystalline Foils

A. Objectives

The objectives of this work are:

(1) To compare the properties of Ta_2O_5 and Nb_2O_5 films under various conditions, in order to determine whether one is intrinsically superior as a dielectric material.
(2) To compare the dielectric properties of Nb_2O_5 films formed on polycrystalline foil, sputtered films, porous plugs and single crystal surfaces, in order to determine the role of grain boundaries in the formation of anodic film defects.
(3) To obtain a better understanding of the reasons for the critical role of anodization conditions (formation electrolyte, temperature, time and current density) in determining dielectric properties of anodic films.

B. Status

(1) Single Crystals

Three cylindrical single crystals of tantalum and two crystals of niobium have been tested for orientation by a back reflection technique. One niobium and one tantalum crystal were oriented in the 110 direction, and the others in the 100 direction. A zone reflection camera has been assembled and is being used to assess the imperfections in these and twelve additional crystals.

Surfaces of both tantalum and niobium crystals have been polished mechanically, electrolytically and chemically, and compared by optical and electron microscopy to determine the optimum surface condition for anodization experiments. Microscopic studies are also being made of their surface topography and structural configurations, using conventional etching techniques.

(2) Polycrystalline Foils

Sections of capacitor-grade niobium and tantalum foils, 1" x 2", have been anodized at 25°C and a constant current of 25 ma, in an electrolyte consisting of 0.01 wt. % H_3PO_4 in demineralized water, according to the schedule listed below:

Specimen No.	Material	Maximum Voltage	Time at Voltage
1	Ta	100	30 minutes
2	Nb	100	30 minutes
3	Ta	150	30 minutes
4	Ta	200	30 minutes
5	Ta	250	30 minutes
6	Ta	300	30 minutes
7	Ta	350	30 minutes
8	Ta	380	5 minutes (scintillated)
9	Ta	100	30 minutes

All specimens were degreased and chemically polished before anodization. A mixture of 2:2:5 parts $HF:HNO_3:H_2SO_4$ by volume was used for polishing specimens 1 to 5; since this solution left the specimens with a dull appearance, the proportions of the acids were altered to 6:4:7 for the other specimens. Direct carbon replicas have been made of the oxide films formed on these specimens and electron micrographs taken.

(3) Transmission Electron Microscopy of Thinned Metallic Foils

A specimen of the capacitor-grade niobium foil has been successfully thinned for transmission electron microscopy. It is hoped that slices of niobium and tantalum single crystals can be similarly thinned for electron microscopy, in order to obtain a more complete picture of their substructures and dislocation patterns.

(4) Transformation of Oxide Films

In order to study the thermal transformations of the "in situ" anodic films, samples of capacitor-grade niobium and tantalum foil were anodized at 25°C to 100 volts at a current density of 1 ma/cm^2 for 30 minutes in 0.01 wt. % H_3PO_4 in demineralized water. The anodized foils were cut into 2 x 4 mm strips and sealed in silica tubes under argon, for heat treatment. Specimens have been heated at 600, 700, 800 and 900°C for two hours, and examined using a 15-degree angle x-ray diffraction technique. By this method, crystallization of the amorphous oxide at these temperatures has been demonstrated. Although the patterns have not yet been completely analyzed, it appears that the crystallite size of the niobium oxide increases more rapidly with increasing temperature than that of the tantalum oxide. Additional heat treatment studies at lower temperatures are in progress.

Growth of crystallites in the amorphous oxide layer can also be induced under the electron beam during electronic microscopic examination, when surface impurities are present. Figure 19 shows the rapid growth which took place on an anodic tantalum film in which small fluoride inclusions were identified. Figure 19 (a) shows the film (16,500x magnification) upon initial exposure to the beam, while Figures 19 (b), (c), and (d) show the same area after 2, 4 and 5 minutes respectively, under the electron beam.

TABLE I

ANALYSES OF NIOBIUM FROM THREE DIFFERENT PROCESSES

MATERIAL:		1 Hydrogen Reduced From Pentachloride		2 Carbon Reduced From Pentoxide		3 Proprietary Process		Detection Method
CONDITION:		As Recd.	H + M 100 M x D*	As Recd.	H + M 100 M x D*	As Recd.	H + M 100 M x D*	
ELEMENT, ppm:	C	30	80	70	110	80	225	(1)
	O	60	1300	2800	2700	650	1500	(2)
	H	71	7500	620	7800	12	6600	(2)
	N	3	170	120	237	25	43	(3)
	B	0.4	0.5	0.4	0.2	0.5	0.3	(4)
	Al	<40[a]	24	<40	<30	<40[a]	<30	(4)
	Ca	<20	<30	20	<30	<20	30	(4)
	Cr	13	19	15	12	11	11	(5)
	Co	<10	< 2	<10	< 2	<10	2	(5)
	Cu	6	6.5	6	7	47	44	(5)
	Fe	130	278	180[b]	67	110	187	(5)
	Li	—	< 1	—	< 1	—	5	(4)
	Mg	<20	<30	<20	<30	<20	<30	(4)
	Mn	< 5	18	< 5	< 5	< 5	< 5	(5)
	Mo	4	6.5	34	36	4	4	(5)
	Ni	15	15	8	14	21	22	(5)
	Si	<50	20	<50	17	<50	140	(4)
	Ta	730	7800	970	1100	320	3500	(5)
							3200	(9)
	Ti	<20[a]	—	25	—	<20[a]	—	(4)
		—	5	—	45	—	9	(7)
	V	—	0.5	—	4	—	< 0.5	(7)
	W	58	176	400	361	< 5	< 5	(5)
	Zr	3	—	0.8	—	1	—	(6)
		—	4	—	10	—	10	(7)
		—	4	—	9	—	15	(8)
	Sn	10	—	< 5	4	15	—	(5)
		—	10	—	4	—	8	(7)

NOTES: H = Hydrided M = Milled * Nominal Size

a = Not detected

b = Average of 4 analyses ranging from 90 to 300 ppm, indicating tramp iron. Magnetic separation was made on the final powder.

Detection Methods: (1) Combustion Conductometric; (2) Vacuum Fusion; (3) Distillation-Spectrophotometric; (4) Emission Spectrographic; (5) Spectrophotometric; (6) Extraction-Emission Spectrographic; (7) Ion Exchange-Emission Spectrographic; (8) Ion Exchange-Spectrophotometric; (9) X-ray Fluorescence.

TABLE 2

ANALYTICAL RESULTS FOR Nb-Ta -200 MESH ALLOY POWDERS

	Nb-Ta Alloy and Nominal Composition			
Element	C (25 wt. % Ta) 4.27 pounds	B (50 wt. % Ta) 4.50 pounds	A (75 wt. % Ta) 4.67 pounds	D (100 wt. % Ta 4.76 pounds
% C	0.010	0.003	0.009	0.013
% O	0.36	0.27	0.17	0.20
% H	0.59	0.51	0.32	0.28
% N	0.058	0.065	0.079	0.039
% Ta	26.3	57.3	80.8	Balance
% Nb	72.2	41.4	18.3	0.96

TABLE 3

LOT ANALYSIS OF NIOBIUM AND TANTALUM -200 MESH POWDERS

TO BE USED FOR PREPARATION OF A SECOND 50% Nb - 50% Ta ALLOY

Material	Lot Number	% C	% O	% N	% H
Niobium	BM 810	0.009	0.25	0.012	0.67
Tantalum	TM 551	0.005	0.21	0.007	—

TABLE 4

PROCESSING DETAILS FOR SMALL BATCHES OF SOLID NIOBIUM CAPACITORS MADE IN ACTIVITY 3

Pressing and Sintering

Powder Blend:	85% -325 mesh, 15% -200/325
Green Density:	4.9 to 5.2 gms/cc
Sintered Density:	4.93 to 5.58 gms/cc
Sintering Temperature:	2100°C
Sintering Time:	30 minutes

Formation

Formation Electrolyte:	Proprietary Y_1 at 25°C
Formation Current Density:	50 ma/gram of niobium material
Formation Voltage V_F:	175 volts
Formation Time at V_F:	5 hours

Impregnation/Reformation

4/5 split dip cycle in $Mn(NO_3)_2$ solution (temperature and composition proprietary).

Pyrolysis Temperature:	275°C with 3 minute conversion time

Reformation in proprietary electrolyte Y_1 at 25°C

First Reformation Voltage V_{RF1}:	70 volts
Second Reformation Voltage V_{RF2}:	65 volts

Carbon and Silver Coating

Standard proprietary method

Canning

Size C cans under proprietary conditions

TABLE 5A

Task A, Activity 3

SOLID TEST MEASUREMENTS OF NIOBIUM CAPACITORS AT 35 VOLTS, 25°C AFTER CANNING BUT BEFORE AGEING

Material and Batch No.	* Description	** No. of Plugs	Cap.(μf) at 120~			D.F.(%) at 120~			Cap.(μf) at 1 kc.			D.F.(%) at 1kc.			Leakage I_L (μa) +			Sintered Density of Plugs
			High	Low	Avg.	High	Low	Avg.	High	Low	Avg.	High	Low	Avg.	High	Low	Avg.	
1 BM 812	(C-10)	10/10	16.60	14.00	14.93	2.4	1.8	2.1	16.47	13.95	14.86	12.19	8.25	10.45	140.00	24.00	60.60	5.58
2 BM 812	(C-11)	1/10			15.00			1.8			14.95			10.67			25.00	5.24
3 BM 812	(C-12)	8/10	14.90	13.40	14.00	2.7	1.7	2.2	14.70	13.22	13.90	14.55	10.39	12.48	80.00	13.00	38.30	5.44
4 BM 812	(C-13)	5/10	13.30	12.00	12.70	2.7	1.6	2.2	13.23	12.02	12.70	13.70	9.55	11.23	8.00	2.90	4.80	5.28
5 BM 812	(C-14)	10/10	16.00	12.30	14.10	2.2	1.5	1.9	16.00	12.30	14.11	10.40	7.98	9.45	600.00	4.30	8.0	5.38
6 BM 812	(C-15)	10/10	15.70	13.70	14.60	4.2	1.7	2.8	15.60	13.73	14.59	12.95	8.48	10.50	30.00	0.70	14.49	5.36
1 2121	(C-10)	5/10	15.40	14.60	15.00	2.5	1.5	1.7	15.33	14.51	14.95	10.62	9.20	9.89	58.00	6.40	23.20	5.26
2 2121	(C-11)	5/10	16.20	14.80	15.60	2.4	1.8	2.1	16.10	14.69	15.40	15.39	11.70	13.22	71.00	12.00	31.80	5.58
3 2121	(C-12)	6/10	15.70	13.30	14.50	2.0	1.6	1.8	15.56	13.29	14.37	11.19	9.70	10.42	34.00	8.40	17.40	5.29
4 2121	(C-13)	8/10	14.20	10.60	12.60	7.6	2.4	3.8	13.88	9.37	12.18	19.05	11.54	12.30	340.00	5.40	11.40	4.93
5 2121	(C-14)	8/8	14.80	12.00	13.40	3.5	2.8	3.2	14.41	11.90	13.18	10.20	7.47	8.41	50.00	3.00	14.5	5.58
6 2121	(C-15)	7/9	16.20	14.20	15.00	2.0	1.4	1.6	16.10	14.13	14.94	9.03	6.02	7.94	15.00	1.70	6.9	5.52

* See flow diagram of Figure I for identification.
** Number of plugs surviving test after canning/number of plugs canned.
\+ Anomalously high leakages omitted from averages.

TABLE 5B

Task A, Activity 3

SOLID TEST MEASUREMENTS OF NIOBIUM CAPACITORS AT 35 VOLTS, 25°C AFTER AGEING AT 35°C, 38 VOLTS FOR 120 HOURS

Material and Batch No.	* Description	** No. of Plugs	Cap. (μf) at 120~			D.F. (%) at 120~			Cap. (μf) at 1kc.			D.F. (%) at 1kc.			Leakage (μa) +		
			High	Low	Avg.	High	Low	Avg.	High	Low	Avg.	High	Low	Avg.	High	Low	Avg.
1 BM 812	(C-10)	9/10	16.40	13.70	14.62	3.17	2.00	2.58	16.23	13.76	14.57	13.73	9.49	11.28	170.00	14.00	62.00
2 BM 812	(C-11)	1/10			14.70			1.65			14.70			10.45			17.00
3 BM 812	(C-12)	8/10	14.60	13.20	13.80	2.30	1.72	1.97	14.49	13.03	13.72	13.00	9.46	11.21	33.00	7.90	19.85
4 BM 812	(C-13)	5/10	13.20	11.80	12.50	2.70	1.76	2.15	12.96	11.80	12.47	13.50	9.53	10.95	12.00	3.50	6.30
5 BM 812	(C-14)	9/10	15.70	12.70	13.79	2.20	1.43	1.73	15.70	12.73	13.79	11.35	9.35	10.27	220.00	2.80	6.73
6 BM 812	(C-15)	10/10	15.40	13.60	14.31	4.00	1.65	2.30	15.33	13.50	14.26	13.20	9.40	10.99	230.00	0.48	6.05
1 2121	(C-10)	5/10	15.20	14.20	14.70	1.90	1.30	1.60	15.20	14.30	14.75	9.18	8.19	8.86	190.00	3.70	11.60
2 2121	(C-11)	5/10	16.00	14.50	15.10	2.44	1.73	2.18	15.83	14.35	15.08	15.72	11.15	13.14	27.00	6.00	16.60
3 2121	(C-12)	6/10	15.50	13.00	14.10	1.92	1.55	1.79	15.39	13.07	14.15	10.55	9.23	10.09	75.00	4.40	30.70
4 2121	(C-13)	8/10	13.70	10.20	12.30	7.60	2.30	3.57	13.48	9.11	11.87	19.10	11.93	14.14	250.00	9.00	23.80
5 2121	(C-14)	8/8	14.60	11.90	13.26	3.95	2.70	3.14	14.22	11.69	12.97	10.74	8.29	9.15	7.60	1.10	2.96
6 2121	(C-15)	7/9	16.00	13.80	14.63	2.32	1.20	1.59	15.82	13.82	14.62	10.65	6.83	9.19	9.20	0.78	4.21

* See flow diagram of Figure I for identification.

** Number of plugs surviving after ageing tests/ number of plugs put on ageing test.

\+ Anomalously high leakages omitted from averages.

TABLE 6

CHEMICAL ANALYSES OF NIOBIUM POWDERS; MATERIAL: LOT BM-818

SUB-ACTIVITY 5.5

Designation	Condition	Where Analyzed	Amount Present, p.p.m.				
			H	O	N	C	Fe
As Received	Partly Hydrided	U.C.M.	600	2700	130	80	-
As Received	Partly Hydrided	Kemet	600	-	-	-	-
As Received	Dehydrided	Kemet	1.7	3600	120	60	50
I-A	Hydrided	Kemet	8800	-	-	-	-
I-B	Hydrided	Kemet	8300	-	-	-	-
II-A	Hydrided	Kemet	8800	-	-	-	-
II-B	Hydrided	Kemet	9200	-	-	-	-
III-A	Hydrided	Kemet	8600	-	-	-	-
III-B	Hydrided	Kemet	9600	-	-	-	-
IV-A	Hydrided	Kemet	8900	-	-	-	-
IV-B	Hydrided	Kemet	8800	-	-	-	-
I-A	Dehydrided	Kemet	5.6	5000	140	100	50
I-B	Dehydrided	Kemet	6.5	5100	150	120	40
II-A	Dehydrided	Kemet	3.7	4400	160	60	30
II-B	Dehydrided	Kemet	3.0	5200	160	60	10
III-A	Dehydrided	Kemet	1.2	4000	120	40	30
III-B	Dehydrided	Kemet	1.5	4700	150	30	10
IV-A	Dehydrided	Kemet	2.6	4600	160	40	30
IV-B	Dehydrided	Kemet	2.1	5200	180	40	10

Nomenclature:

I = -400 mesh "control" powder, not prefurnaced.
II = -400 mesh powder, prefurnaced.
III = -200/+325 mesh powder, prefurnaced.
IV = powder blend, prefurnaced.

A = washing treatment in 30% HNO_3 solution followed by removal of fines.
B = etch treatment in 10% bromine-methanol solution.

TABLE 7

DISTRIBUTION OF POWDER PARTICLE SIZES AS DETERMINED BY MICROMEROGRAPH

	Amount Present, in Per Cent, in Various Sieve Sizes for Designated Powders							
	Distribution	-400mesh(-37μ)		-400mesh(-37μ)		-200/325 Mesh, 74/44μ		Blend, -74μ	
T.S.N.*	Microns	I-A	I-B	II-A	II-B	III-A	III-B	IV-A	IV-B
140	105	-	-	-	-	9	5	1	-
170	88	-	-	-	-	21	16	2	1
200	74	-	-	-	-	23	19	4	4
230	62	-	-	-	-	27	35	13	12
270	53	2	3	-	1	13	14	19	20
325	44	12	7	6	9	4	5	16	17
400	37	18	14	16	17	1	2	14	13
	31	18	24	17	18	1	2	7	10
	26	15	24	19	16	1	-	6	7
	22	11	8	14	13	-	1	6	5
	18.5	8	7	10	9	-	-	4	3
	15.6	5	6	7	7	-	1	4	3
	13.1	4	3	4	3	-	-	2	2
	11.0	3	2	3	2	-	-	1	1
	9.2	1	1	2	2	-	-	-	1
	7.8	1	1	1	1	-	-	1	1
	6.6	1	-	1	1	-	-	-	-
	5.5	1	-	-	1	-	-	-	-
	4.7								
	Geometric Mean, Microns	23.8	24.4	22.2	22.9	63.6	58.8	35.5	34.8

* T.S.N. = Equivalent Tyler Sieve Number

TABLE 8

POROSIMETER RESULTS FROM ANODES OF VARIOUS NIOBIUM POWDERS

PRESSED TO SEVERAL DENSITIES

Plug Designation	Density gm/cc	Total Porosity Per Cent	% of Total Porosity as a Function of Apparent Pore Diameter, μ							Average Pore Size (μ)	Calculated Surface Area cm^2 *
			>15	15-10	10-7	7-5	5-3	3-1.5	<1.5		
I-A-X		56.5	-	-	5	55	32	5	3	5.3	105
I-A-Y	5.65	27.5	-	-	4	26	61	6	3	4.8	112
I-A-Z	6.22	18.9	-	-	-	7	75	14	4	3.7	101
I-B-Y	5.71	36.6	-	-	-	13	57	26	4	3.9	111
II-A-X	4.96	35.4	-	-	6	70	19	3	2	5.7	105
II-A-Y	5.25	28.6	-	-	-	5	78	15	2	4.1	110
II-A-Z	5.80	21.6	-	-	-	-	80	16	4	3.8	105
II-B-Y	5.46	41.1	-	-	-	12	56	25	7	3.7	111
III-A-X	4.83	44.5	77	9	5	3	2	2	2	>15.0	73.5
III-A-Y	5.63	40.1	22	28	27	11	5	4	3	10.0	73.0
III-A-Z	6.38	26.1	-	5	25	45	15	6	4	6.3	66.5
III-B-Y	5.40	43.4	20	25	31	11	5	4	4	9.8	74.7
IV-A-X	4.91	42.8	10	13	42	20	11	3	1	8.0	89.0
IV-A-Y	5.39	41.8	-	-	16	49	26	7	2	5.5	97.5
IV-A-Z	6.21	23.2	-	-	-	7	75	15	3	3.7	90.5
IV-B-Y	5.40	47.2	-	5	7	46	32	5	5	5.1	98.5

* Calculated from Wet Capacitance Measurements Using $C = \frac{AK}{36\pi \cdot 10^5 \cdot t}$

where K = dielectric constant
A = area in cm^2
t = dielectric thickness in cm
C = capacitance in μf

TABLE 9

RESULTS OF WET ELECTRICAL TESTS OF SEVERAL ANODES FROM NIOBIUM POWDER, LOT BM-818

(TERMINAL LEAKAGE CURRENTS MEASURED IN Y-1, OTHER WET TESTS IN 30% H_2SO_4)

Plug Designation	Weight grams	Density g/cc	Capacitance and Dissipation Measurements *								D-C Leakage, at 25°C			
			120 cps Test				1000 cps Test				150 Volts		200 Volts	
			Ω	S	S^1	D.F.(%)	Ω	S	S^1	D.F.(%)	µa/µf	µa/S^1	µa/µf	µa/S^1
I-A-X	0.361	4.98	3.61	18.0	294	1.38	3.57	17.8	291	9.08	-	-	22.3	0.61
I-A-Y	0.432	5.65	3.22	18.2	298	1.20	3.21	18.1	297	8.73	1.58	0.045	11.3	0.32
I-A-Z	0.484	6.22	2.58	16.1	264	1.64	2.56	15.9	261	11.58	-	-	25.5	0.74
I-B-Y	0.428	5.71	3.23	18.4	302	1.20	3.23	18.5	303	6.71	1.04	0.027	9.8	0.29
II-A-X	0.338	4.96	3.86	19.1	314	0.94	3.86	19.1	314	5.33	0.99	0.025	18.1	0.46
II-A-Y	0.374	5.25	3.65	19.2	314	1.06	3.65	19.2	314	6.85	0.65	0.017	17.3	0.46
II-A-Z	0.426	5.80	3.07	17.8	292	1.41	3.05	17.7	290	10.18	0.69	0.019	18.6	0.51
II-B-Y	0.389	5.46	3.55	19.4	318	1.14	3.54	19.4	317	7.09	0.65	0.017	14.9	0.39
III-A-X	0.397	4.83	2.30	11.1	182	0.82	2.31	11.1	183	4.65	0.70	0.021	16.9	0.52
III-A-Y	0.468	5.63	1.94	10.9	179	0.80	1.94	10.9	179	4.80	0.48	0.015	16.9	0.53
III-A-Z	0.540	6.38	1.53	9.78	160	0.88	1.53	9.76	160	5.74	0.67	0.021	20.4	0.64
III-B-Y	0.446	5.40	2.08	11.3	184	0.77	2.09	11.3	185	4.86	0.53	0.016	14.7	0.45
IV-A-X	0.366	4.91	3.03	14.9	244	0.78	3.02	14.9	243	4.45	0.61	0.017	15.1	0.42
IV-A-Y	0.426	5.39	2.85	15.4	252	0.78	2.84	15.3	251	6.14	0.58	0.017	14.6	0.43
IV-A-Z	0.500	6.21	2.25	14.0	229	1.03	2.25	14.0	229	6.56	0.75	0.022	19.5	0.59
IV-B-Y	0.421	5.40	2.91	15.7	258	0.99	2.91	15.7	257	6.22	0.50	0.015	12.9	0.37

LEGEND: Ω = charge number in milli-coulombs/g S = size factor in milli-coulombs/cc
S^1 = size factor in milli-coulombs/in^3

* Formation voltage V_F = 200 volts at 25°C. The Ω, S, S^1 values have been normalized to the equivalent formation voltage at 90°C = 164 volts.

TABLE 10

MnO_2 CONTENT OF PLUGS AS A FUNCTION OF THE NUMBER OF DIPS IN MnO_2 AND OF PYROLYSIS TEMPERATURE

Pyrolysis Temperature	Number of $Mn(NO_3)_2$ Dips	Weighing Method		Analytical Method	
		Average Total MnO_2 Buildup Milligrams	Average MnO_2 Pickup in Pores Milligrams	Total Mn Content in Pores Milligrams	Calculated MnO_2* Content in Pores Milligrams
275°C	1	10.3	6.2	6.6	10.4
	2	16.5	11.5	10.0	15.8
	4	38.1	24.8	16.3	25.8
	6	56.8	31.0	21.4	33.9
	8	73.5	34.0	24.6	39.0
	10	84.5	42.1	28.2	44.6
350°C	2	16.3	12.2	9.3	14.7
	4	37.2	21.1	15.5	24.5
	6	62.0	31.1	21.1	33.4
	8	80.5	35.8	24.7	39.0
	10	92.2	40.0	26.5	41.9
425°C	2	20.3	15.3	11.2	17.7
	4	41.3	20.4	16.3	25.8
	6	64.9	31.2	21.2	33.6
	8	87.5	37.2	25.9	40.9
	10	117.1	40.9	26.1	41.3

* Calculated from total Mn content on the assumption of complete stoichiometry.

TABLE 11A

Sub-Activity 5.5

LEAKAGE CURRENT MEASUREMENTS FOR CANNED NIOBIUM CAPACITORS BEFORE AGEING

Batch No.	Pyrolysis Temp. °C	Avg. Preheat Temp.	Conv. Time Mins.	No. of Dips $Mn(NO_3)_2$	Leakage Current – μA												No. of Survivors at 35 V
					12 Volts			15 Volts			25 Volts			35 Volts			
					High	Low	Avg.	High	Low	Avg.	High	Low	Avg.	High	Low	Avg.	
1A	275	265	3½	8				0.081	0.015	0.048	0.75	0.45	0.60	1.7	1.0	1.35	2/4
1B	275	–	3½	8				1.0	0.036	0.199	2.30	0.16	0.71	9.8	0.57	3.55	7/9
2A	275	*	3½	4/4				3.5	0.110	0.86	10.0	0.33	2.76	27.0	1.2	7.72	5/5
2B	275	–	3½	4/4				0.22	0.025	0.104	0.63	0.06	0.281	1.4	0.29	0.747	9/9
3A	275	*	3½	10				0.78	0.78	0.78	2.7	2.7	2.7	7.3	7.3	7.3	1/5
3B	275	–	3½	10				15.0	0.15	5.0	53.0	0.65	16.4	33.0	1.7	13.4	5/10
4A	275	*	3½	5/5				0.21	0.14	0.20	1.7	1.2	1.43	4.5	3.6	3.97	3/5
4B	275	–	3½	5/5				1.0	0.15	0.415	9.3	1.0	3.68	68.0	5.2	25.3	6/10
5A	350	353	3½	8				–	–	–	–	–	–	–	–	–	0/5
5B	350	–	3½	8				0.29	0.29	0.29	1.9	1.9	1.9	4.2	4.2	4.2	1/10
6A	350	332	3½	4/4				3.4	3.4	3.4	12.0	12.0	12.0	36.0	36.0	36.0	1/5
6B	350	–	3½	4/4				1.6	0.15	0.67	19.0	0.75	7.96	100.0	3.0	34.83	4/10
7A	350	348	3½	10				0.25	0.25	0.25	5.0	5.0	5.0	33.0	33.0	33.0	1/5
7B	350	–	3½	10				–	–	–	–	–	–	–	–	–	0/10
8A	350	334	3½	5/5				0.59	0.25	1.38	2.7	1.0	1.8	19.0	2.7	9.4	3/5
8B	350	–	3½	5/5				5.3	1.4	2.7	34.0	3.6	19.32	94.0	9.8	49.96	5/10
9A	425	422	3½	8				–	–	–	–	–	–	–	–	–	0/5
9B	425	–	3½	8				19.0	18.0	18.5	150.0	100.0	125.0	620.0	370.0	495.0	2/10
10A	425	416	3½	4/4				–	–	–	–	–	–	–	–	–	0/5
10B	425	–	3½	4/4				52.0	6.9	21.98	190.0	31.0	91.0	550.0	130.0	282.0	5/10
11A	225	225	3½	4/4	0.080	0.010	0.030	Unsteady			0.57	0.14	0.428	2.6	0.65	1.39	5/5
11B	225	–	3½	4/4	0.019	0.006	0.010	0.024	0.006	0.011	0.17	0.023	0.067	0.78	0.07	0.31	5/5
12	225	–	5	4/4	0.18	0.007	0.047	0.24	0.007	0.070	1.10	0.031	0.377	4.1	0.085	1.16	5/5
13A	250	236	3½	4/4	3.10	0.004	0.889	4.4	0.012	1.370	9.70	0.077	4.113	28.0	0.20	9.68	5/5
13B	250	–	3½	4/4	2.00	0.002	0.575	3.5	0.008	0.988	13.00	0.047	3.704	34.0	0.14	9.56	5/5
14	250	–	5	4/4	0.093	0.015	0.045	0.059	0.019	0.041	1.5	0.25	0.73	7.4	1.0	3.4	3/5

Not Measured

* Temperature was not measured with thermocouple, but average value same (265°C) as for Batch 1A.

TABLE 11B

Sub-Activity 5.5

CAPACITANCE AND DISSIPATION FACTOR MEASUREMENTS FOR CANNED NIOBIUM CAPACITORS BEFORE AGEING

Batch No.	Pyrolysis Temp. °C	Avg. Preheat Temp.	Conv. Time Mins.	No. of Dips $Mn(NO_3)_2$	C & D Measured at 120 cps, 12 volts						C & D at 1000 cps 12 Volts Avg. Only	
					Capacitance - µF			Dissipation - %				
					High	Low	Avg.	High	Low	Avg.	C - µF	D.F.-%
1A	275	265	3½	8	13.0	12.1	12.6	2.2	1.9	2.1		
1B	275	-	3½	8	13.7	11.0	12.6	3.0	2.1	2.5		
2A	275	Not Measured*	3½	4/4	14.2	12.4	13.2	1.9	1.5	1.7	Not Measured	Not Measured
2B	275	-		4/4	13.2	12.0	12.6	2.0	1.5	1.7		
3A	275	Not Measured*	3½	10	13.3	11.6	12.2	1.5	1.2	1.4		
3B	275	-	3½	10	12.8	10.9	11.9	1.7	1.3	1.5		
4A	275	Not Measured*	3½	5/5	14.3	13.6	13.9	1.8	1.3	1.6		
4B	275	-	3½	5/5	13.8	12.3	13.1	2.5	1.7	2.1		
5A	350	353	3½	8	18.0	17.0	17.6	1.9	1.4	1.6	17.5	6.0
5B	350	-	3½	8	17.7	15.6	16.6	1.7	1.4	1.5	16.6	6.1
6A	350	332	3½	4/4	16.9	16.4	16.7	1.9	1.7	1.8	16.6	8.1
6B	350	-	3½	4/4	15.9	14.7	15.4	1.8	1.5	1.6	15.3	7.2
7A	350	348	3½	10	17.8	17.4	17.6	1.8	1.7	1.8	17.5	7.0
7B	350	-	3½	10	16.4	14.6	15.6	1.9	1.5	1.7	15.4	6.0
8A	350	334	3½	5/5	16.8	15.2	15.7	1.7	1.4	1.5	15.7	6.0
8B	350	-	3½	5/5	15.6	15.2	15.3	2.0	1.4	1.6	15.2	6.0
9A	425	422	3½	8	16.2	13.4	14.8	11.0	1.2		15.1	6.8
9B	425	-	3½	8	17.4	13.7	16.4	54.0	1.4		15.7	
10A	425	416	3½	4/4	26.5	19.8		43.0	5.3		20.6	13.7
10B	425	-	3½	4/4	16.9	8.7	14.3	1.7	1.3	1.5	14.2	6.8
11A	225	225	3½	4/4	9.7	9.3	9.6	1.9	1.3	1.5	9.5	6.5
11B	225	-	3½	4/4	9.8	8.8	9.2	3.0	1.5	2.2	8.9	9.6
12	225	-	5	4/4	10.1	9.6	9.8	2.9	2.4	2.7	9.3	13.1
13A	250	236	3½	4/4	10.6	10.1	10.2	1.7	1.3	1.5	10.3	7.2
13B	250	-	3½	4/4	10.4	9.4	9.8	2.5	1.6	2.2	9.6	10.9
14	250	-	5	4/4	10.8	10.0	10.3	1.7	1.5	1.6	10.1	8.4

* Approximately 265°C

TABLE 12

BREAKDOWN VOLTAGE MEASUREMENTS AT 25°C FOR NIOBIUM FOIL SPECIMENS IN DIFFERENT ELECTROLYTES

Electrolyte	Conductivity at 25°C $(ohm\text{-}cm)^{-1} \times 10^4$	Avg. B.D.* (J = 1) (Volts)	dv/dt** (J = 1) Volts/Min.	Avg. B.D.* (J = 10) (Volts)	Electrolyte	Conductivity at 25°C $(ohm\text{-}cm)^{-1} \times 10^4$	Avg. B.D.* (J = 1) (Volts)	dv/dt Volts/Min.
H_3PO_4	3.41	259	11.6	243	X_1	3.41	334	14.9
Borcol	3.35	173	18.5	308	X_2	1.71	347	14.7
Y_1	3.46	430	16.0	430	X_3	4.15	301	15.1
Acetic	3.46	154	11.8	230	X_4	7.63	298	13.5
Nitric	3.41	114	13.8	118	X_5	13.2	287	13.7
Y_2	1.38	391	16.0	388	X_6	1.01	312	15.7
KOH	3.38	147	13.4	223	X_7	0.571	350	14.3
Succinic	3.40	156	13.0	212	X_8	0.323	360	15.2
Malonic	3.42	127	13.7	212	X_9	0.182	211	15.1
Y_3	14.9	337	10.3	376	Y_4	0.926	498	15.6
Oxalic	3.41	155	13.8	185	Y_5	0.654	491	15.2
NH_4NO_3	3.33	127	14.1	123	Y_6	11.7	367	16.3
NH_4OH	3.41	174	12.4	250	Y_7	0.247	517	15.9
Arsenic	3.41	182	13.5	233	Y_8	0.083	455	16.0
$HgSO_4$	3.41	170	13.1	-	Y_9	0.05	343	16.8

* J = formation current density = 1 ma/cm^2 or 10 ma/cm^2.
** dv/dt = slope of linear portion of v-t characteristic up to breakdown

TABLE 13

BREAKDOWN VOLTAGE AT 90°C FOR NIOBIUM FOIL SPECIMENS IN DIFFERENT ELECTROLYTES

Electrolyte	Formation Current Density J ma/cm^2	Average B.D.V. Volts	Average dv/dt Volts/Min.	Electrolyte	Formation Current Density J ma/cm^2	Average B.D.V. Volts	Average dv/dt Volts/Min.
H_3PO_4	1	120	10.9	Y_3	1	230	12.4
Y_1	1	210	12.4	Y_3	10	300	118.0
Y_1	10	300	106.0	Y_7	1	217	12.2

TABLE 14

BREAKDOWN VOLTAGES FOR FOILS FORMED IN ONE ELECTROLYTE, ETCHED TO REMOVE THE OXIDE LAYER AND THEN REANODIZED IN ELECTROLYTE Y_1

All Formations at t = 25°C and J = 1 ma/cm^2

First Formation Electrolyte	Maximum Attainable Voltage in First Electrolyte (Volts)	$V_{B.D.}$ in Y_1 (Volts)	First Formation Electrolyte	Maximum Attainable Voltage in First Electrolyte (Volts)	$V_{B.D.}$ in Y_1 (Volts)
Acetic	169	340	Phosphoric	257	350
Nitric	120	362	Y_1	352	330
Nitric	102	350	Y_2	404	300
Malonic	127	350	Y_3	340	330
Ammonium Nitrate	127	360			

TABLE 15

WET TESTS OF LEAKAGE CURRENT, CAPACITANCE AND DISSIPATION FACTOR FOR NIOBIUM FOIL SPECIMENS

Tests in Formation Electrolyte		Tests in 30% H_2SO_4 at 25°C		
Formation Electrolyte E_F	Average Terminal Leakage Current I_T $\mu a/cm^2$	Average Capacitance C/A $\mu F/cm^2$	Average Dissipation Factor D. F. %	Average Leakage Current at 75 Volts $\mu a/cm^2$
Y_1	16.0	0.0495	1.28	1.02
Y_3	14.3	0.0503	1.39	1.08
Y_7	13.7	0.0498	0.83	0.37

FIGURE 1

FLOW DIAGRAM FOR TREATMENT OF A NIOBIUM MATERIAL TO STUDY OPTIMUM PROCESSING FOR REMOVAL OF CARBON

Activity 3

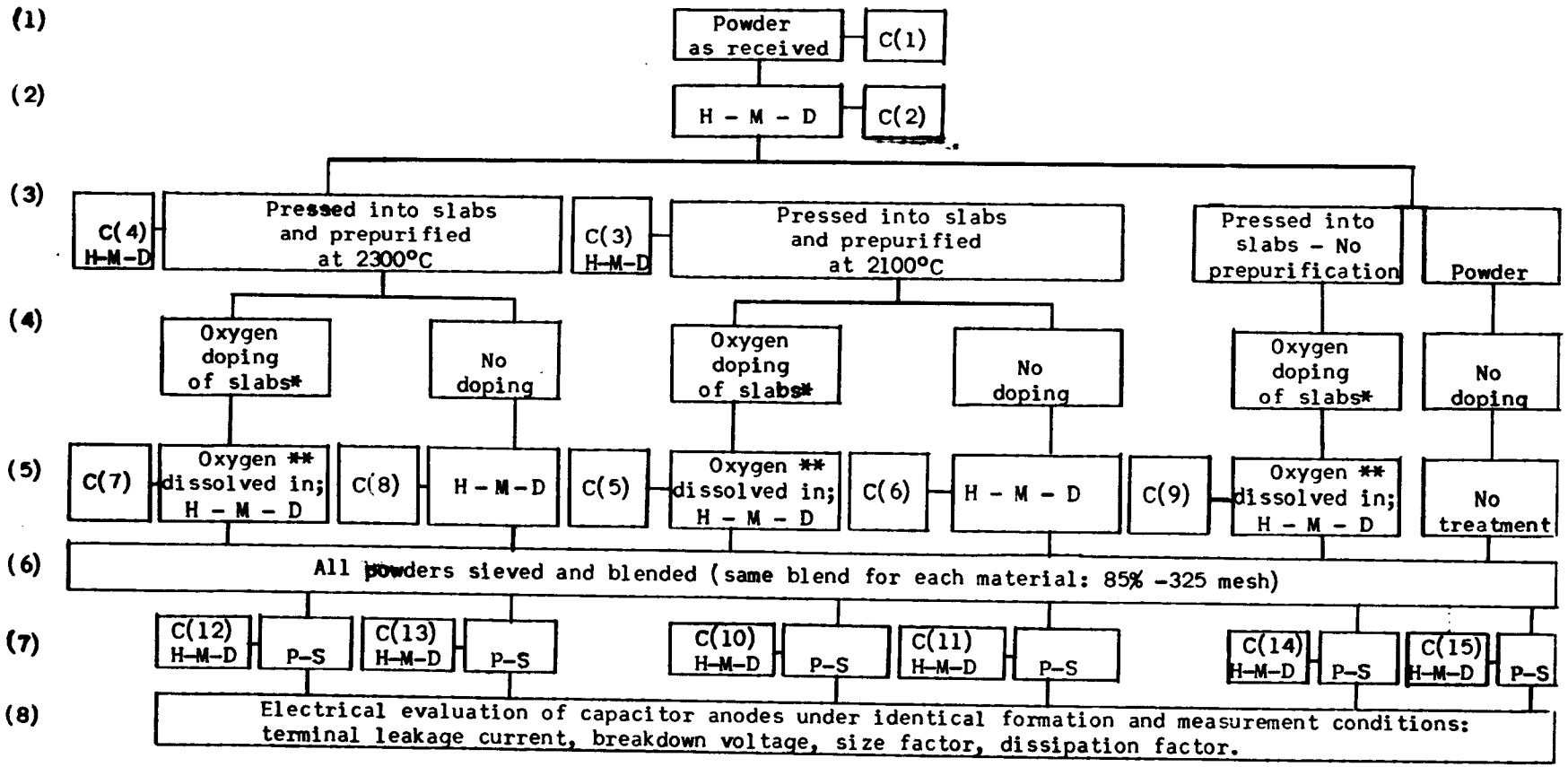

C(i) = sample taken for chemical analysis for C, O, Fe, N; samples H-M-D to obtain -100 mesh powder.
H = hydrogenation; M = ball milling in argon atmosphere; D = high vacuum dehydriding;
P = pressing into capacitor plugs of minimum green density (0.160" diameter, 0.320" long);
S = sintering of anodes in high vacuum at 2100°C for thirty minutes.
* = controlled oxygen doping by electrochemical anodization.
** = surface layer of oxygen dispersed uniformly into metal by vacuum diffusion at 1000°C.

FIG. 2

Variation of Breakdown Voltage of Nb Plugs with Conductivity of Formation Electrolyte

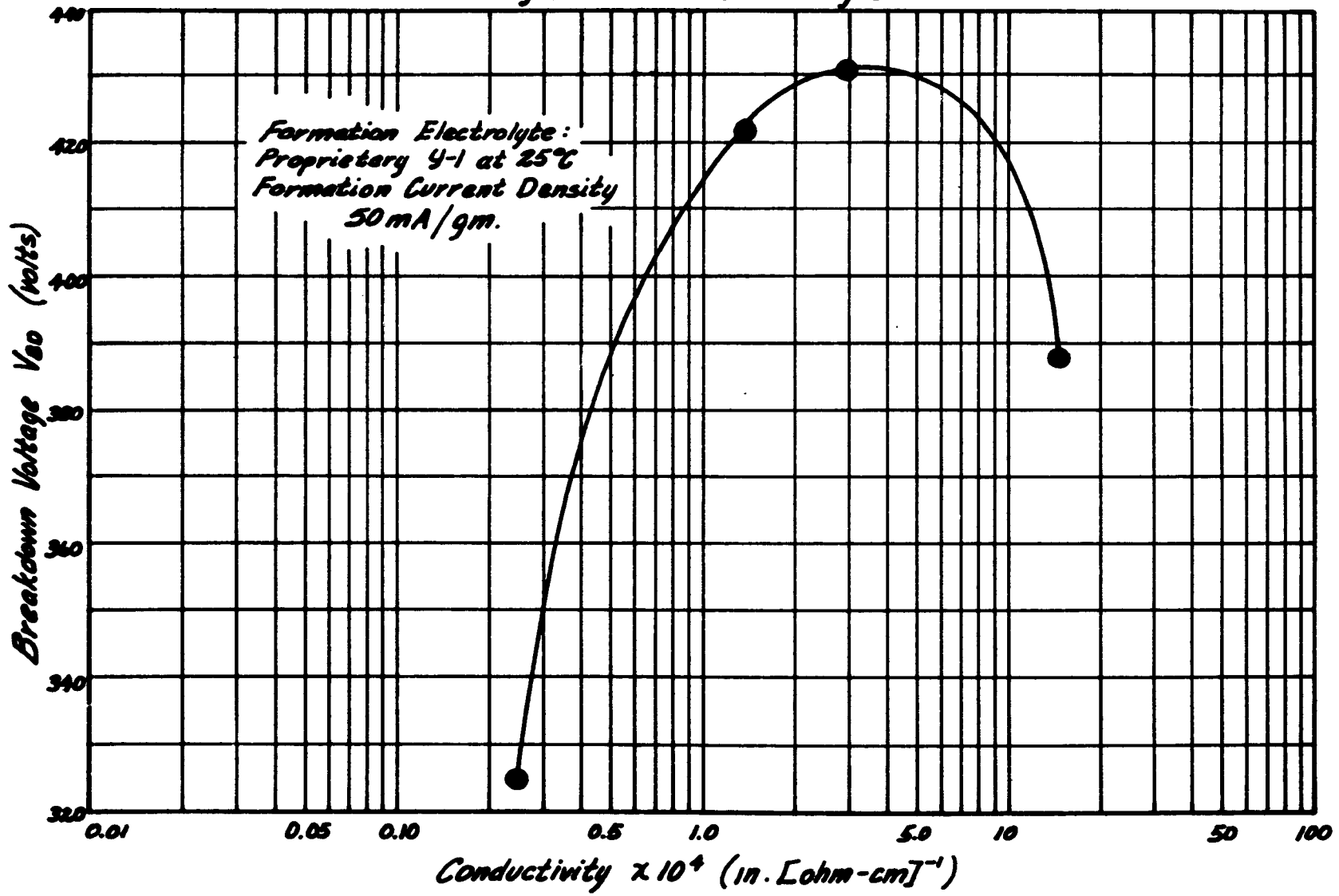

FIG. 3

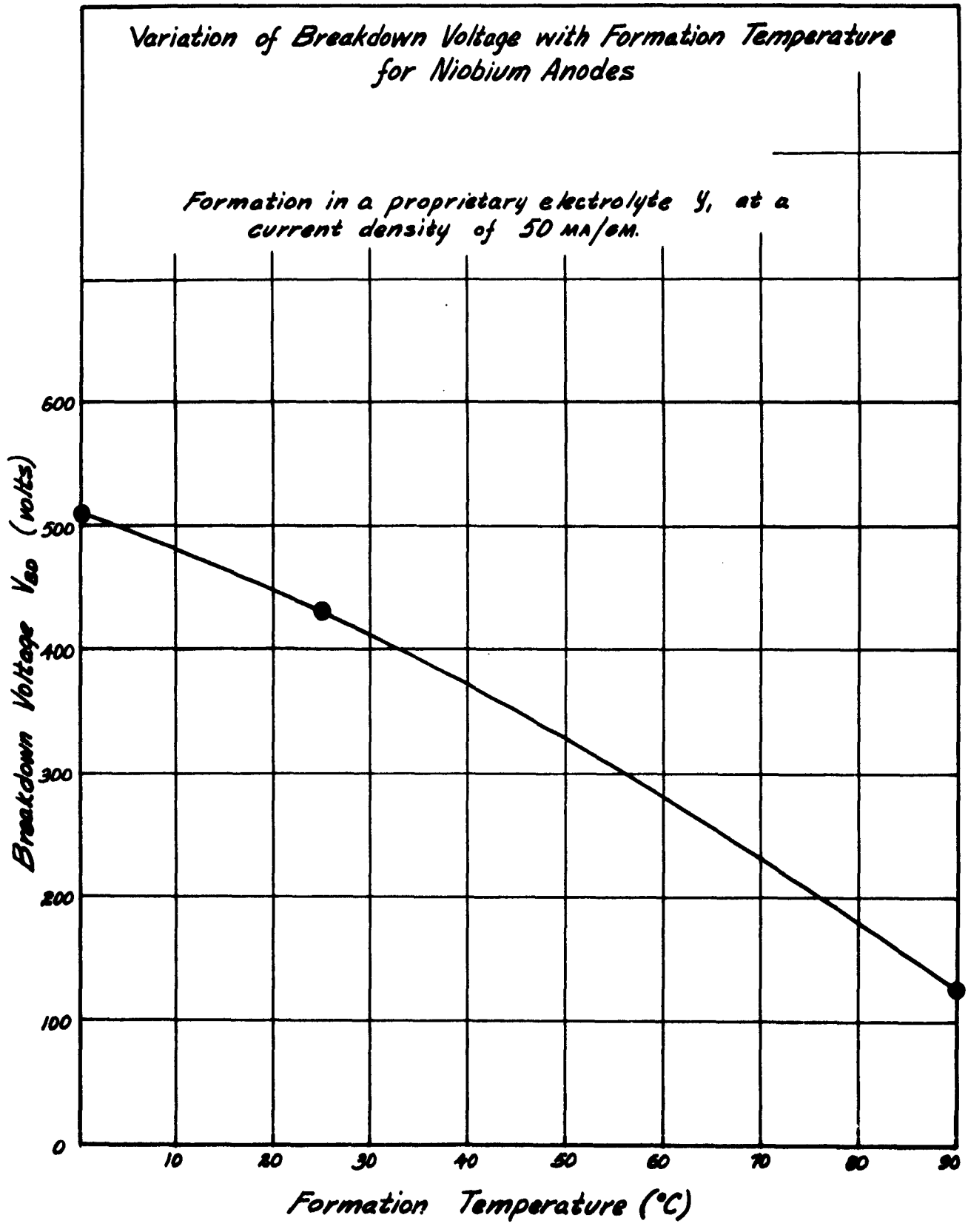
Variation of Breakdown Voltage with Formation Temperature for Niobium Anodes
Formation in a proprietary electrolyte Y, at a current density of 50 MA/CM.
Breakdown Voltage V_{BD} (volts)
0
100
200
300
400
500
600
10
20
30
40
50
60
70
80
90
Formation Temperature (°C)

FIG. 4

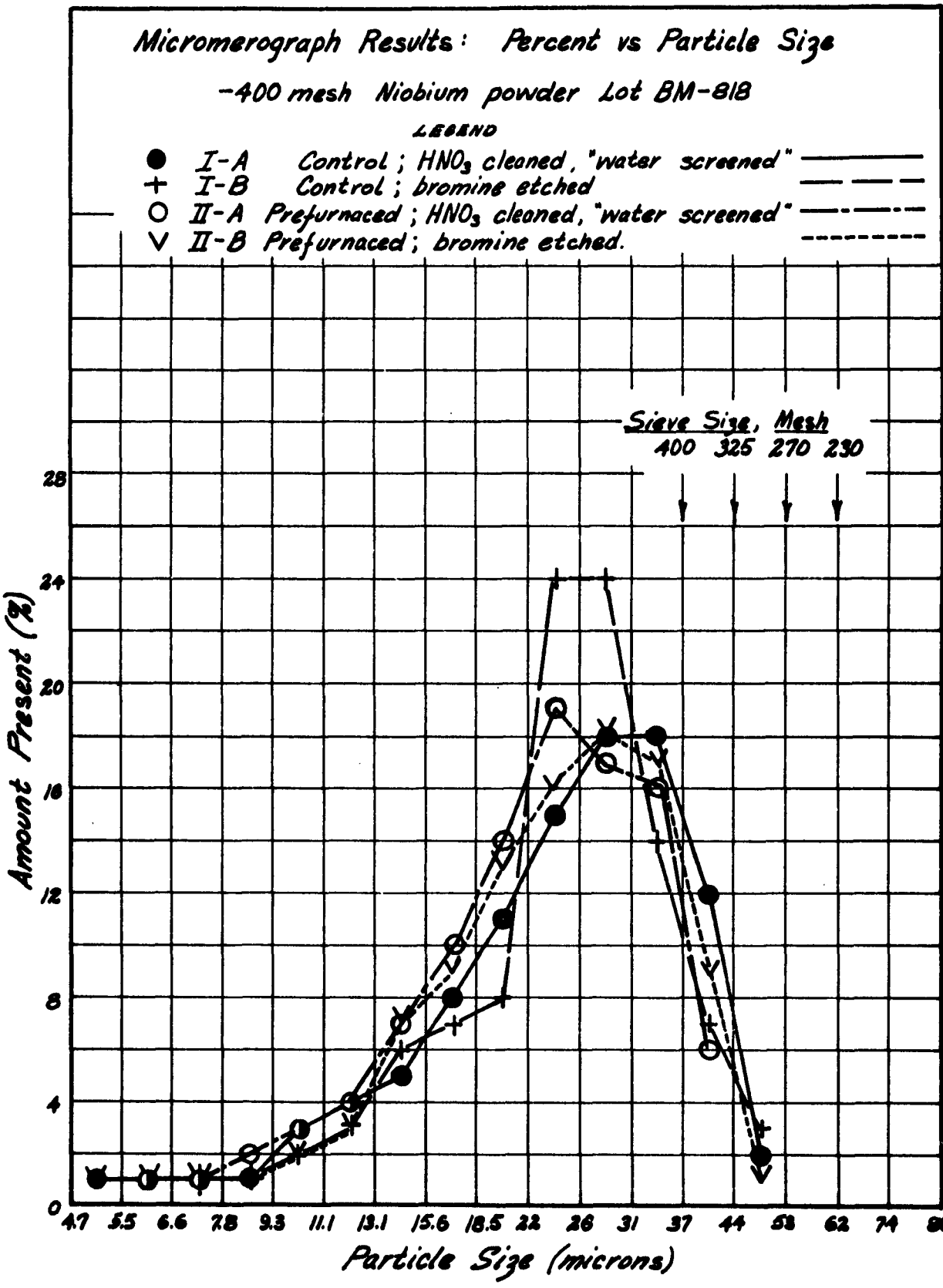
Micromerograph Results: Percent vs Particle Size
-400 mesh Niobium powder Lot BM-818
LEGEND
I-A Control; HNO3 cleaned, "water screened"
I-B Control; bromine etched
II-A Prefurnaced; HNO3 cleaned, "water screened"
II-B Prefurnaced; bromine etched.
Sieve Size, Mesh
400 325 270 230
Amount Present (%)
0
4
8
12
16
20
24
28
4.7 5.5 6.6 7.8 9.3 11.1 13.1 15.6 18.5 22 26 31 37 44 53 62 74 88
Particle Size (microns)

FIG. 5

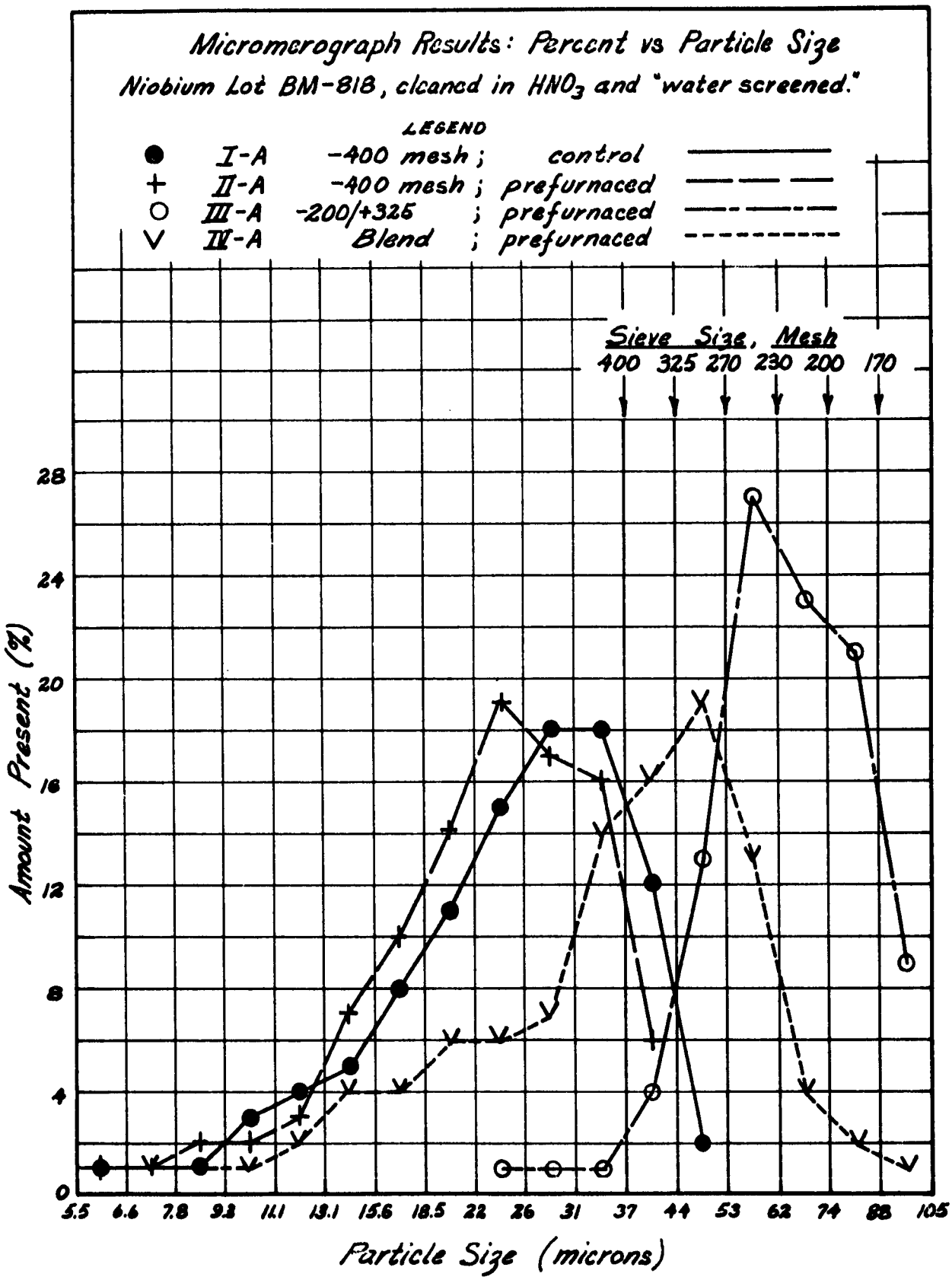
Micromcrograph Results: Percent vs Particle Size
Niobium Lot BM-818, cleaned in HNO3 and "water screened."
LEGEND
I-A -400 mesh; control
II-A -400 mesh; prefurnaced
III-A -200/+325; prefurnaced
IV-A Blend; prefurnaced
Sieve Size, Mesh
400 325 270 230 200 170
Amount Present (%)
0 4 8 12 16 20 24 28
5.5 6.6 7.8 9.3 11.1 13.1 15.6 18.5 22 26 31 37 44 53 62 74 88 105
Particle Size (microns)

FIG. 6

Typical Apparent Pore Diameter Distributions

● Plugs II-A-X Blend Sintered Density : 4.91 gm/cc ; Percent pores 42.8

\+ Plugs II-A-Y Blend Sintered Density : 5.39 gm/cc ; Percent pores 41.8

○ Plugs II-A-Z Blend Sintered Density : 6.21 gm/cc ; Percent pores 23.2

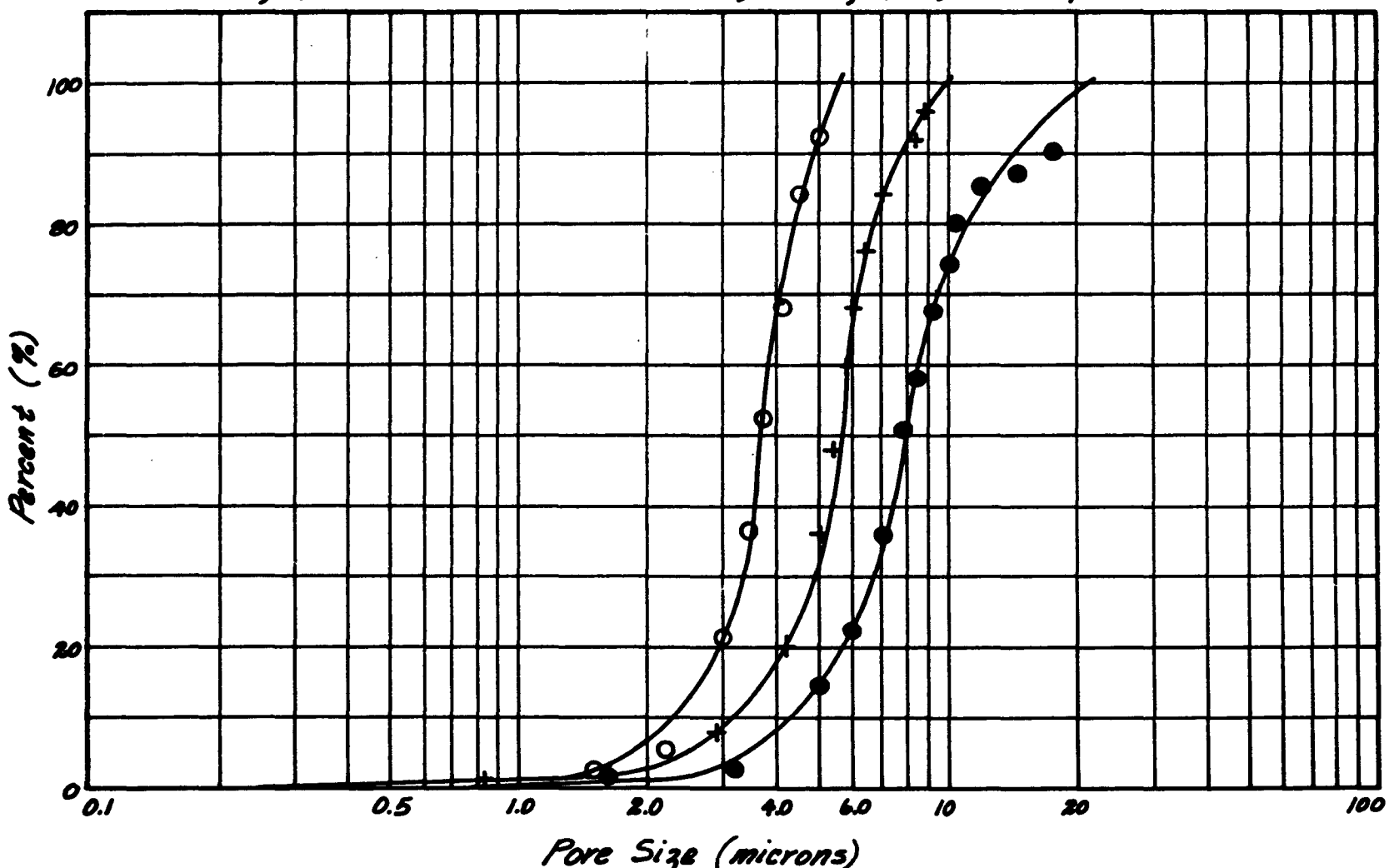

FIG. 7

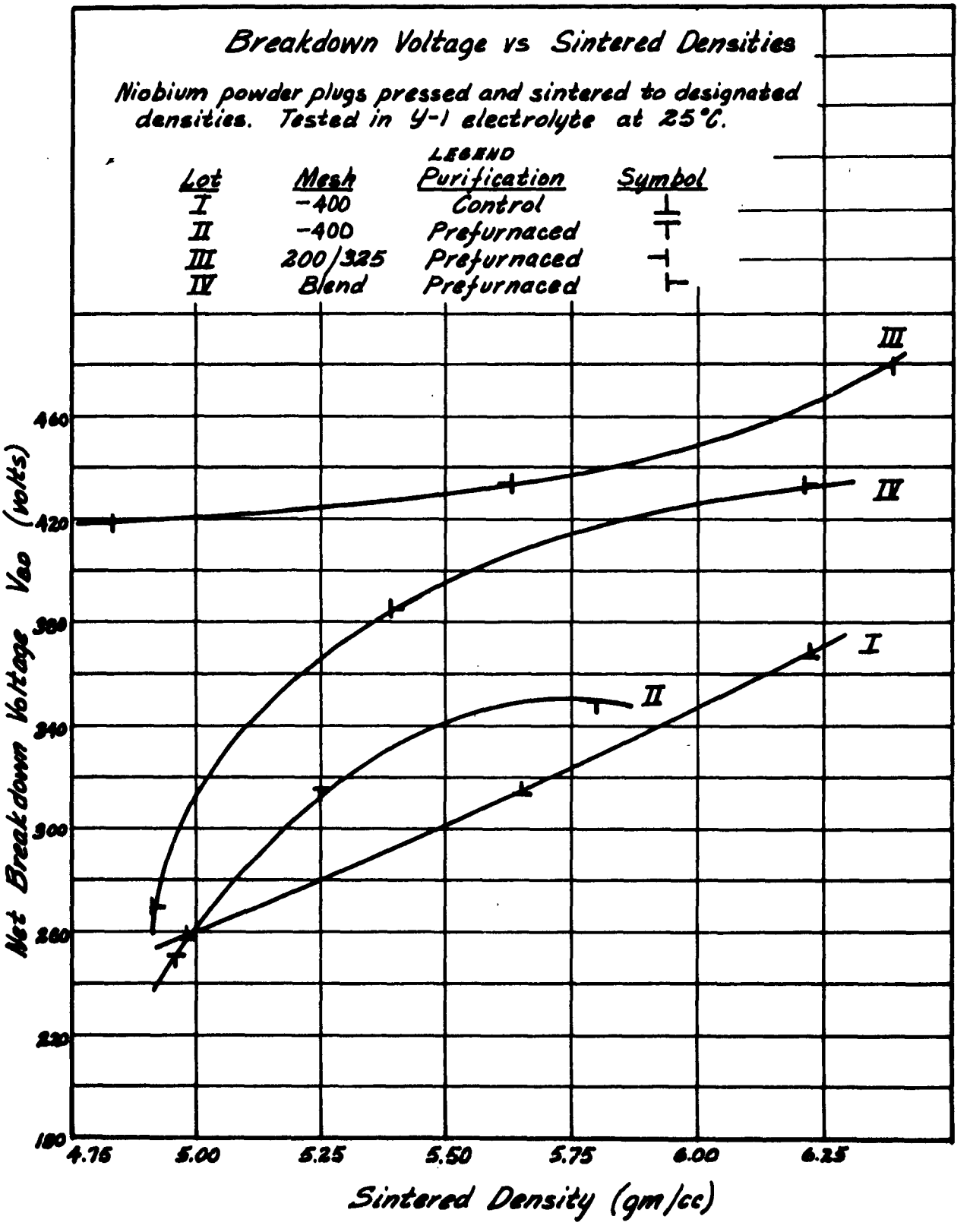
Breakdown Voltage vs Sintered Densities
Niobium powder plugs pressed and sintered to designated densities. Tested in Y-1 electrolyte at 25°C.
LEGEND
Lot | Mesh | Purification | Symbol
I | -400 | Control
II | -400 | Prefurnaced
III | 200/325 | Prefurnaced
IV | Blend | Prefurnaced
III
II
I
460
420
380
340
300
260
220
180
4.76
5.00
5.25
5.50
5.75
6.00
6.25
Net Breakdown Voltage V80 (volts)
Sintered Density (gm/cc)

FIG. 8

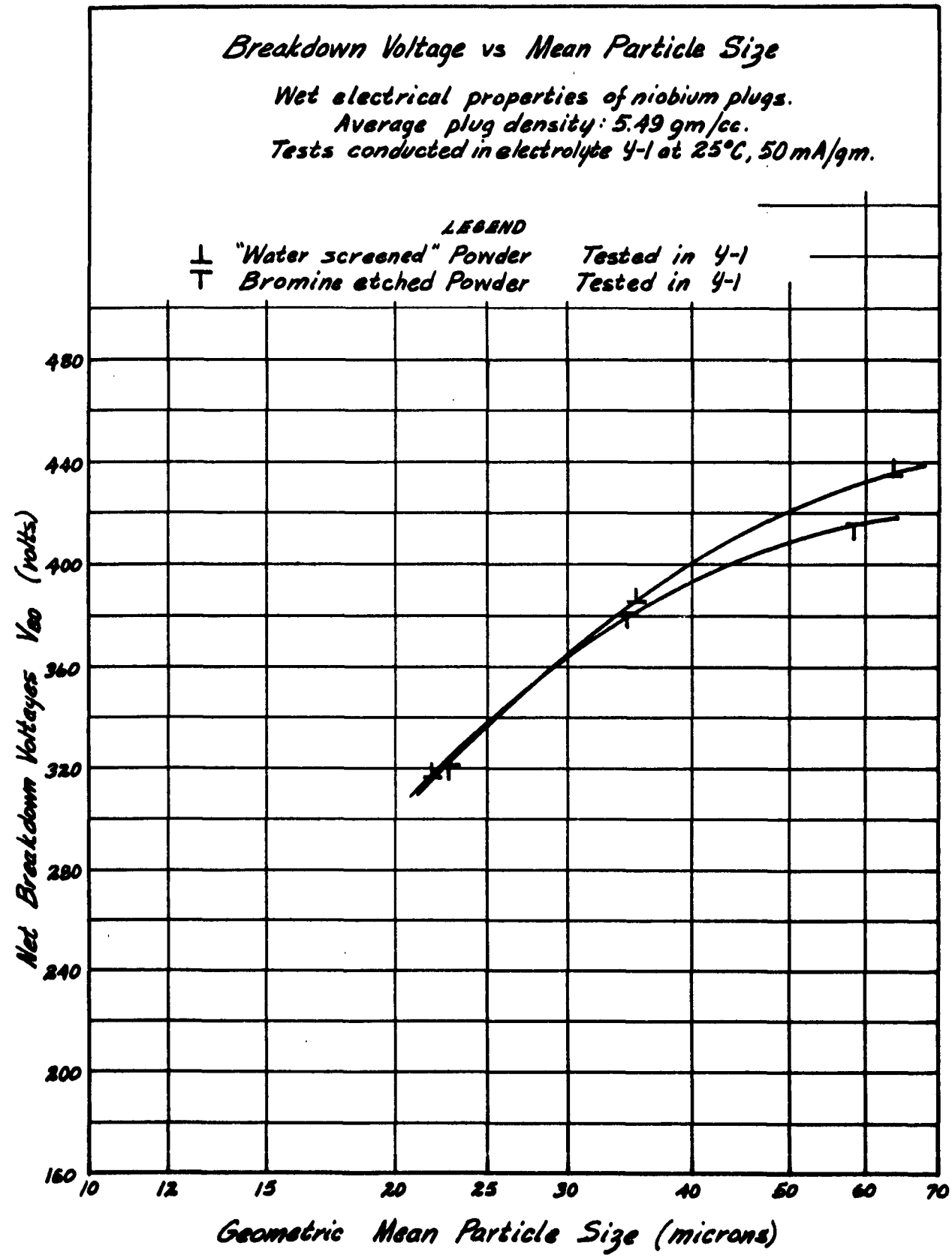
Breakdown Voltage vs Mean Particle Size
Wet electrical properties of niobium plugs.
Average plug density: 5.49 gm/cc.
Tests conducted in electrolyte 4-1 at 25°C, 50 mA/gm.
LEGEND
"Water screened" Powder Tested in 4-1
Bromine etched Powder Tested in 4-1
480
440
400
360
320
280
240
200
160
Net Breakdown Voltages V80 (volts)
10
12
15
20
25
30
40
50
60
70
Geometric Mean Particle Size (microns)

FIG. 9

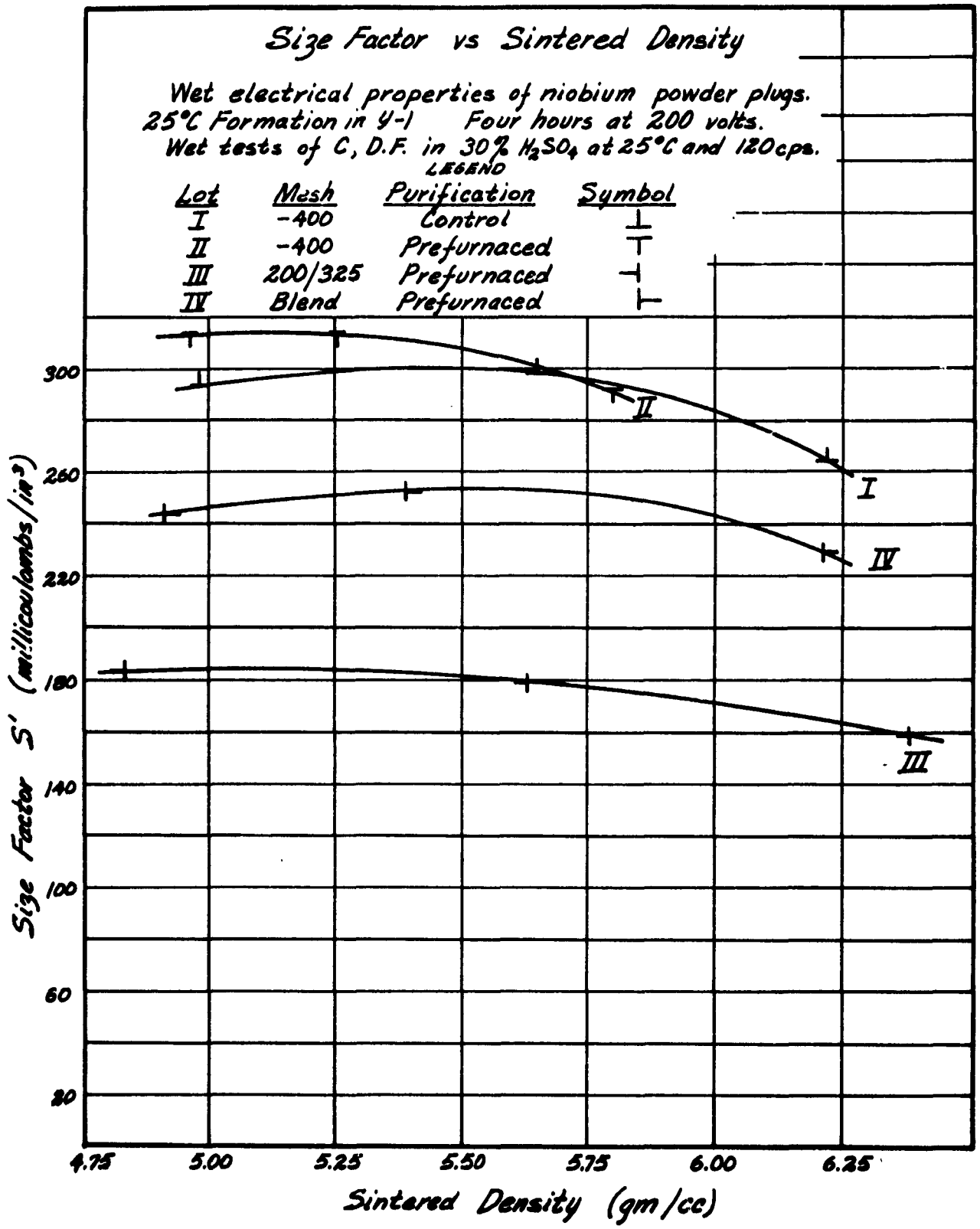
Size Factor vs Sintered Density
Wet electrical properties of niobium powder plugs.
25°C Formation in 4-1 Four hours at 200 volts.
Wet tests of C, D.F. in 30% H2SO4 at 25°C and 120cps.
LEGEND
Lot Mesh Purification Symbol
I -400 Control
II -400 Prefurnaced
III 200/325 Prefurnaced
IV Blend Prefurnaced
300
260
220
180
140
100
60
20
Size Factor S' (millicoulombs/in²)
4.75
5.00
5.25
5.50
5.75
6.00
6.25
Sintered Density (gm/cc)
I
II
III
IV

FIG. 10

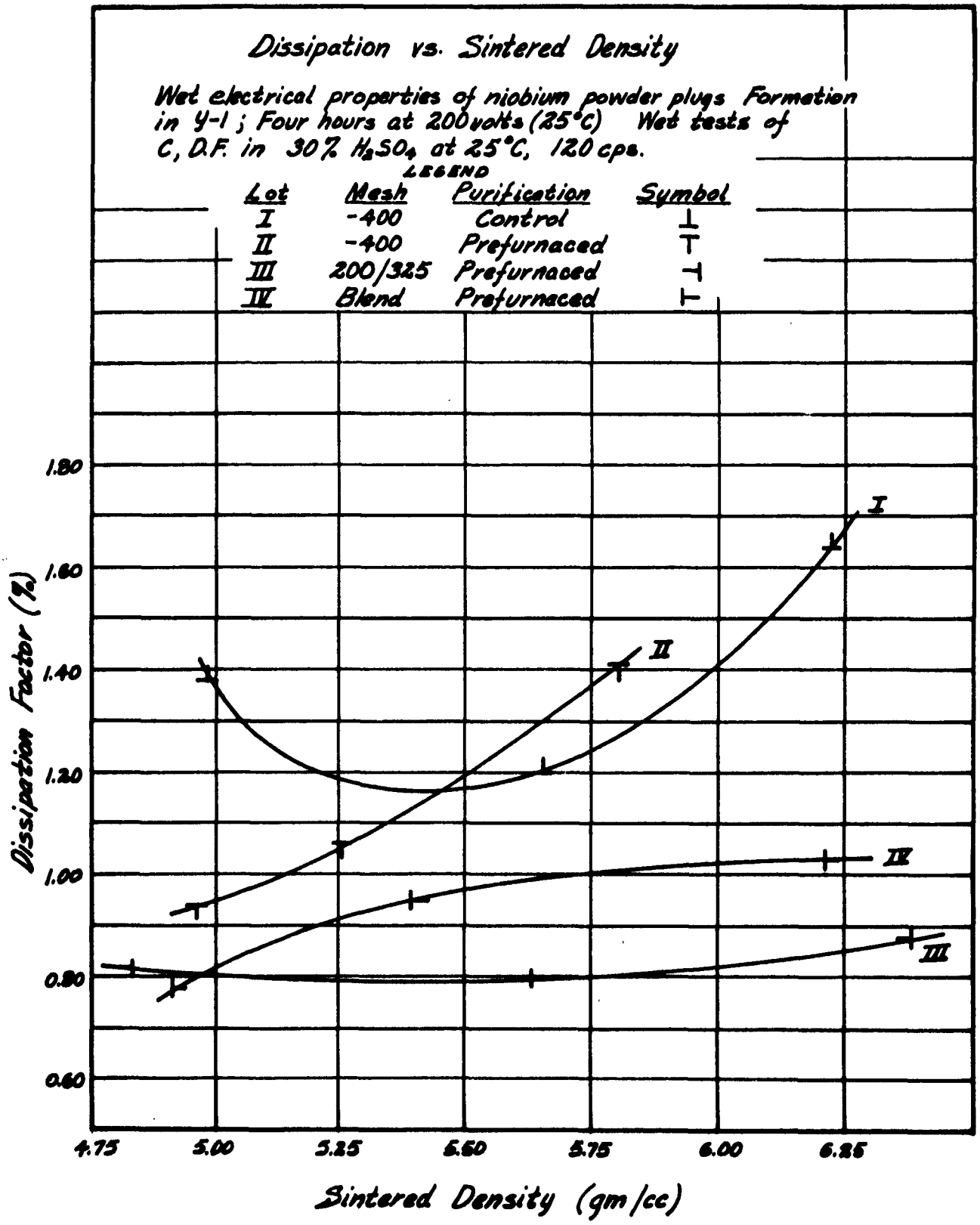
Dissipation vs. Sintered Density
Wet electrical properties of niobium powder plugs Formation in 4-1; Four hours at 200 volts (25°C) Wet tests of C, D.F. in 30% H_2SO_4 at 25°C, 120 cps.
LEGEND
Lot | Mesh | Purification | Symbol
I | -400 | Control
II | -400 | Prefurnaced
III | 200/325 | Prefurnaced
IV | Blend | Prefurnaced
Dissipation Factor (%)
1.80
1.60
1.40
1.20
1.00
0.80
0.60
4.75
5.00
5.25
5.50
5.75
6.00
6.25
Sintered Density (gm/cc)
I
II
III
IV

FIG. 11

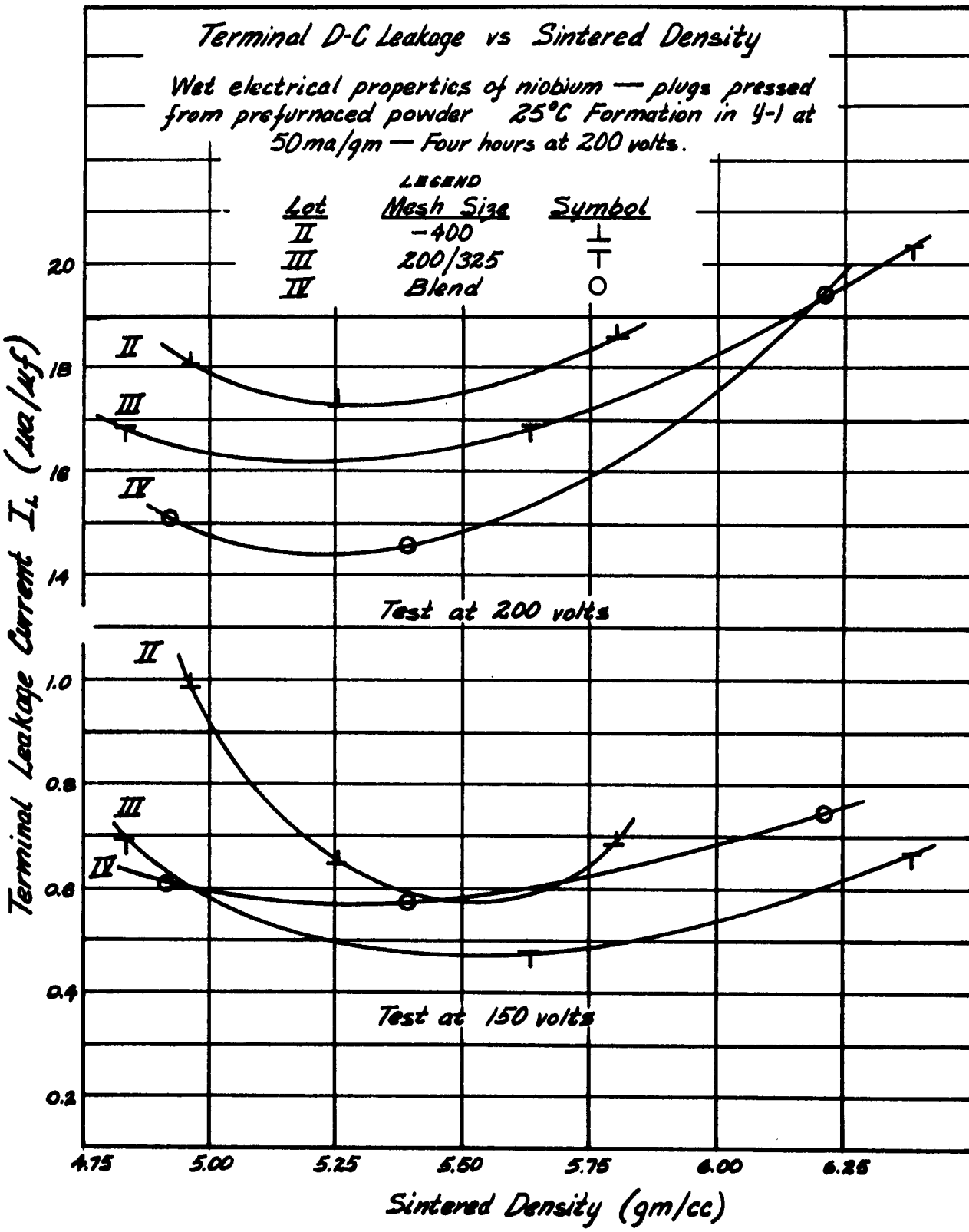
Terminal D-C Leakage vs Sintered Density
Wet electrical properties of niobium — plugs pressed from prefurnaced powder 25°C Formation in 4-1 at 50 ma/gm — Four hours at 200 volts.
LEGEND
Lot
Mesh Size
Symbol
II
-400
III
200/325
IV
Blend
Test at 200 volts
Test at 150 volts
Terminal Leakage Current I_L (μa/μf)
Sintered Density (gm/cc)
20
18
16
14
1.0
0.8
0.6
0.4
0.2
4.75
5.00
5.25
5.50
5.75
6.00
6.25

FIG. 12

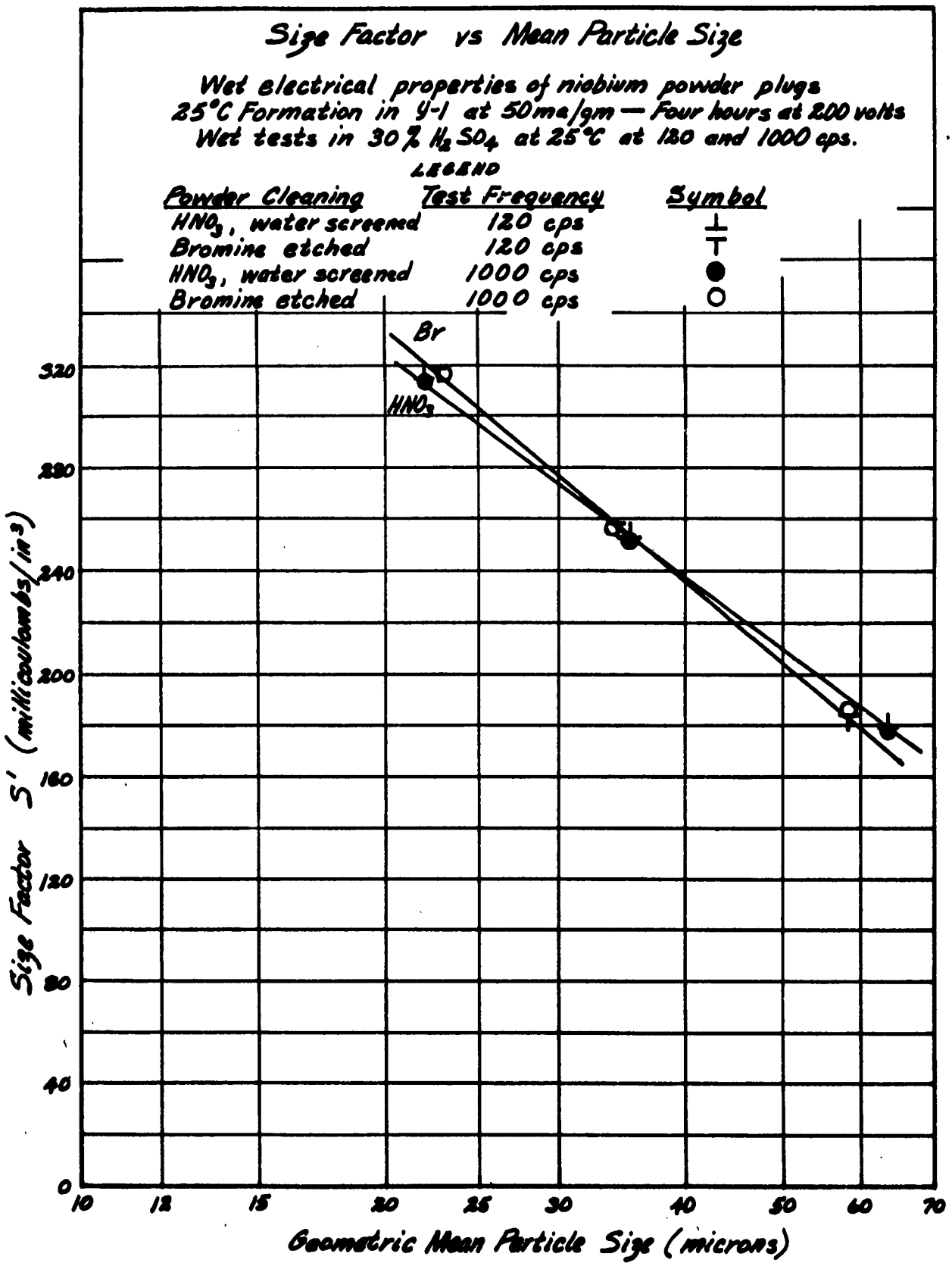
Size Factor vs Mean Particle Size
Wet electrical properties of niobium powder plugs
25°C Formation in 4-1 at 50 ma/gm — Four hours at 200 volts
Wet tests in 30% H_2SO_4 at 25°C at 120 and 1000 cps.
LEGEND
Powder Cleaning
Test Frequency
Symbol
HNO_3, water screened
120 cps
⊥
Bromine etched
120 cps
T
HNO_3, water screened
1000 cps
●
Bromine etched
1000 cps
○
Br
HNO_3
320
280
240
200
160
120
80
40
0
Size Factor S' (millicoulombs/in²)
10
12
15
20
25
30
40
50
60
70
Geometric Mean Particle Size (microns)

FIG. 13

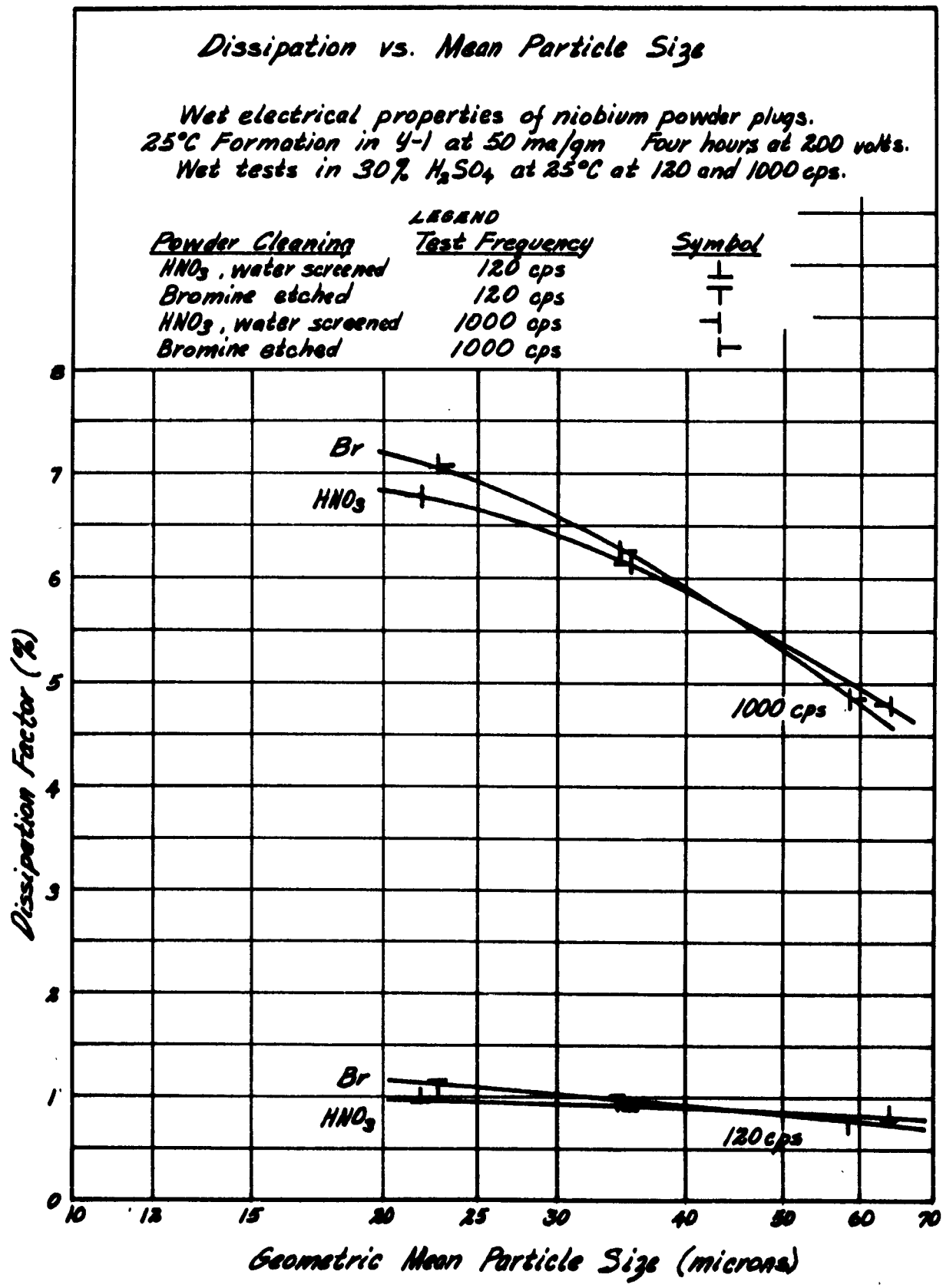
Dissipation vs. Mean Particle Size
Wet electrical properties of niobium powder plugs.
25°C Formation in 4-1 at 50 ma/gm Four hours at 200 volts.
Wet tests in 30% H_2SO_4 at 25°C at 120 and 1000 cps.
LEGEND
Powder Cleaning
Test Frequency
Symbol
HNO_3, water screened 120 cps
Bromine etched 120 cps
HNO_3, water screened 1000 cps
Bromine etched 1000 cps
Br
HNO_3
1000 cps
Br
HNO_3
120 cps
Dissipation Factor (%)
0
1
2
3
4
5
6
7
8
10
12
15
20
25
30
40
50
60
70
Geometric Mean Particle Size (microns)

FIG. 14.

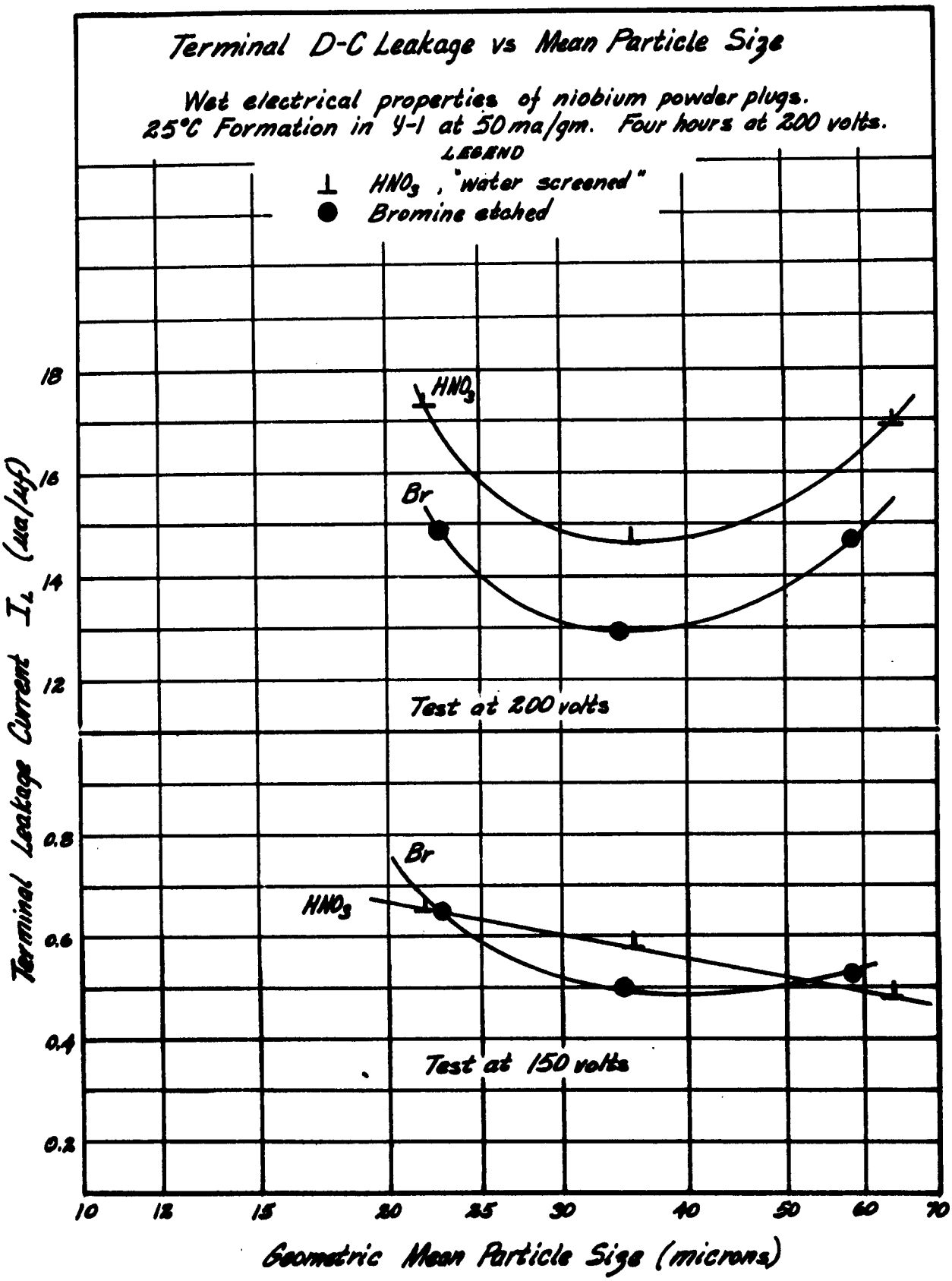
Terminal D-C Leakage vs Mean Particle Size
Wet electrical properties of niobium powder plugs.
25°C Formation in 4-1 at 50 ma/gm. Four hours at 200 volts.
LEGEND
⊥ HNO3, "water screened"
● Bromine etched
HNO3
Br
Test at 200 volts
Br
HNO3
Test at 150 volts
Terminal Leakage Current IL (μa/μf)
18
16
14
12
0.8
0.6
0.4
0.2
10
12
15
20
25
30
40
50
60
70
Geometric Mean Particle Size (microns)

FIG. 15

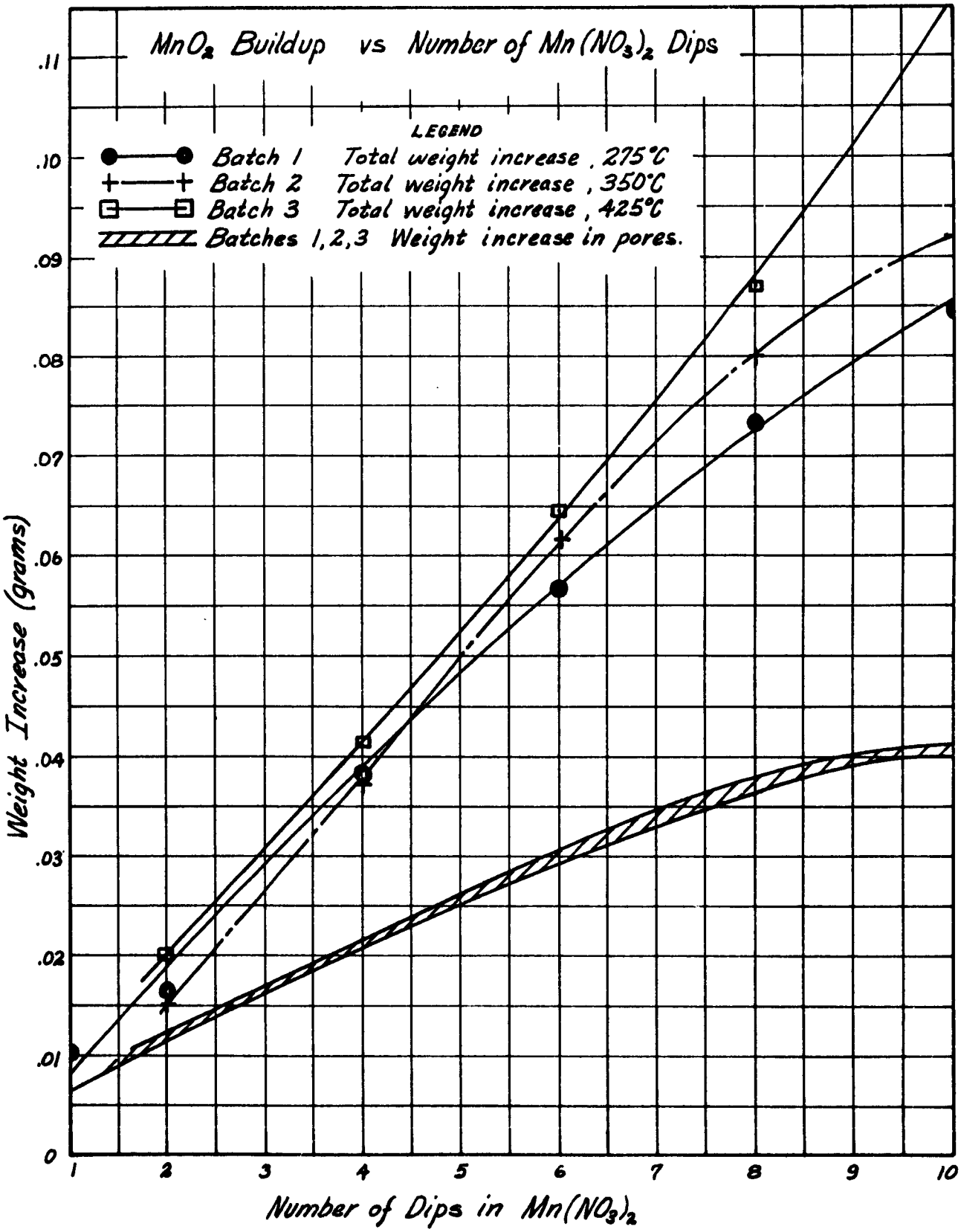
MnO_2 Buildup vs Number of $Mn(NO_3)_2$ Dips
LEGEND
Batch 1 Total weight increase, 275°C
Batch 2 Total weight increase, 350°C
Batch 3 Total weight increase, 425°C
Batches 1,2,3 Weight increase in pores.
Weight Increase (grams)
0
.01
.02
.03
.04
.05
.06
.07
.08
.09
.10
.11
1
2
3
4
5
6
7
8
9
10
Number of Dips in $Mn(NO_3)_2$

FIG. 16

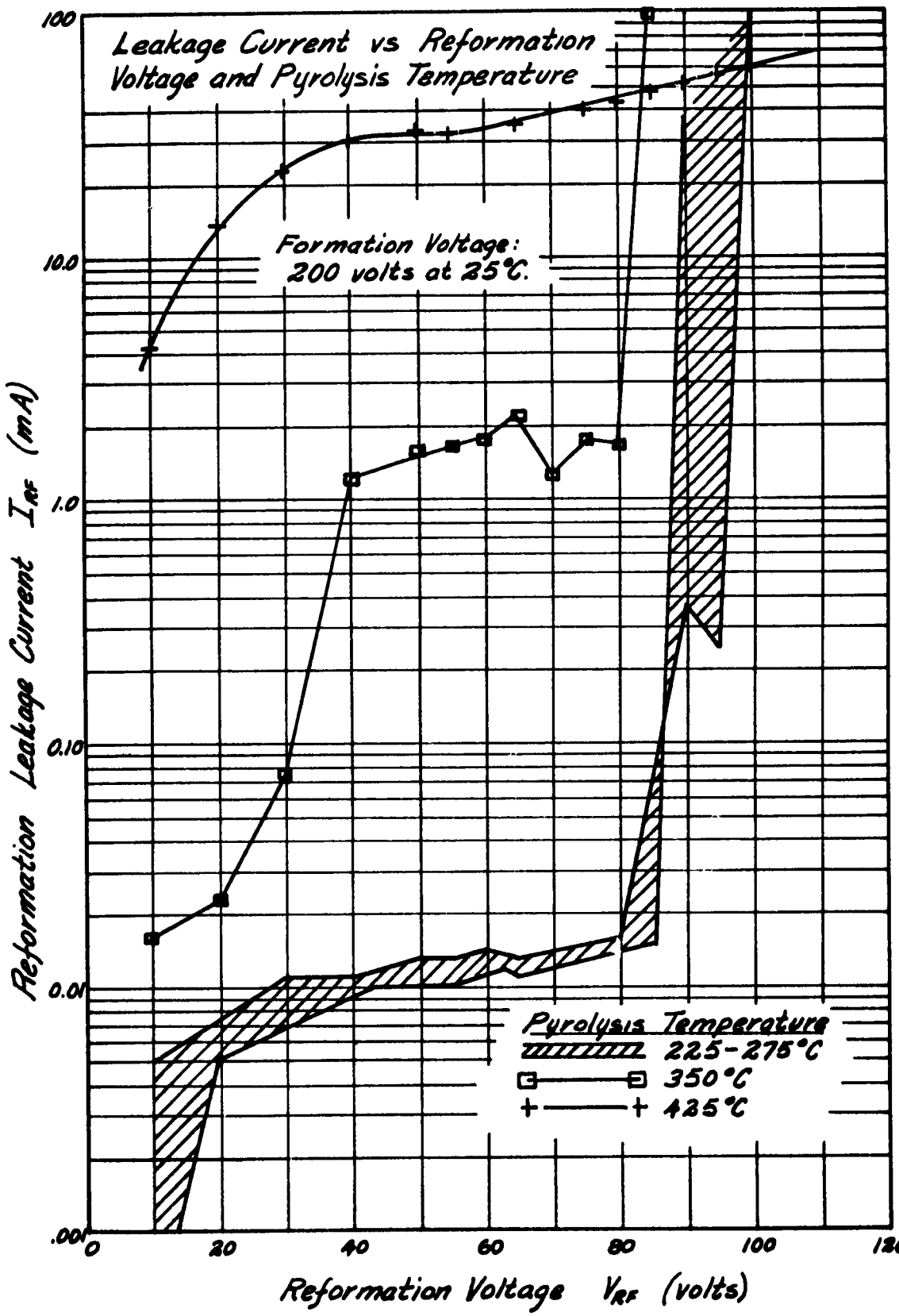
Leakage Current vs Reformation Voltage and Pyrolysis Temperature
Formation Voltage: 200 volts at 25°C.
Pyrolysis Temperature
225-275°C
350°C
425°C
Reformation Leakage Current I_{RF} (mA)
100
10.0
1.0
0.10
0.01
.001
0
20
40
60
80
100
120
Reformation Voltage V_{RF} (volts)

FIG. 17

Percent Failures vs Life Test Time at 85°C for 12 µf/35 volt Solid Niobium Capacitors.

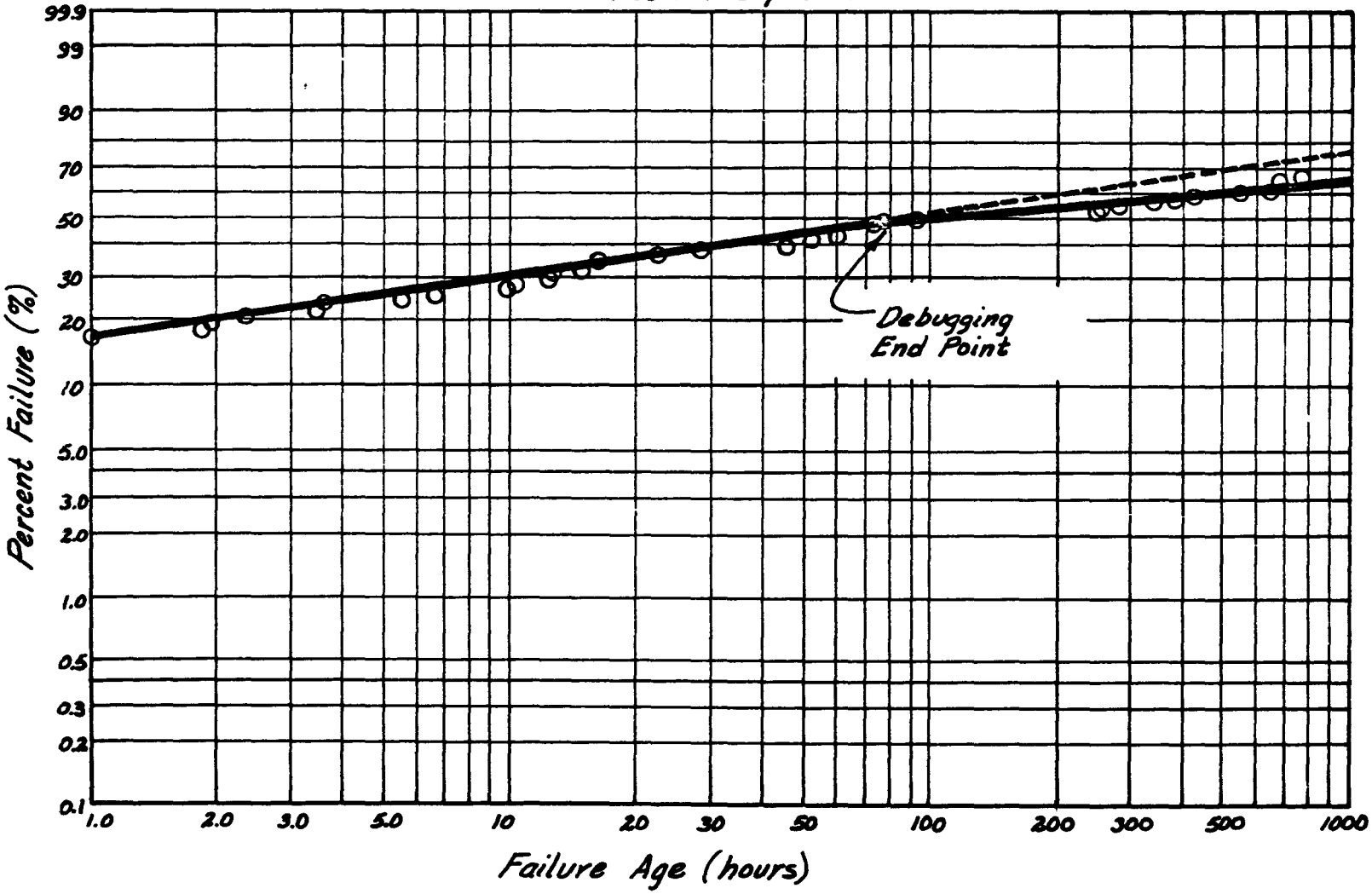

FIG. 18

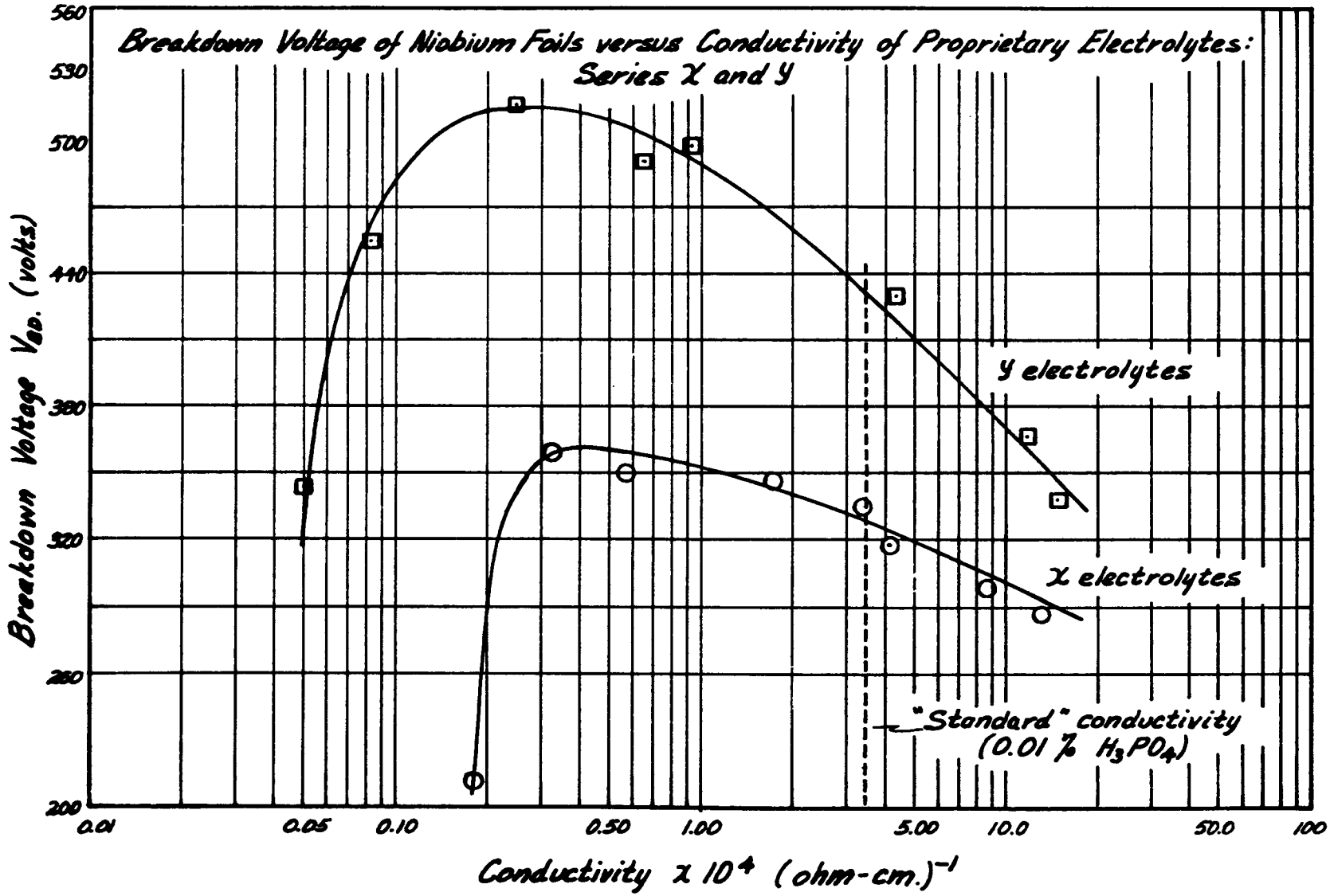
Breakdown Voltage of Niobium Foils versus Conductivity of Proprietary Electrolytes: Series X and Y
Breakdown Voltage V_{BD}. (volts)
560
530
500
440
380
320
260
200
0.01
0.05
0.10
0.50
1.00
5.00
10.0
50.0
100
Conductivity x 10^4 (ohm-cm.)$^{-1}$
Y electrolytes
X electrolytes
"Standard" conductivity
(0.01 % H_3PO_4)

FIGURE 19

ELECTRON BEAM INDUCED TRANSFORMATION
FROM AMORPHOUS TO CRYSTALLINE STATE
IN AN ANODIC FILM

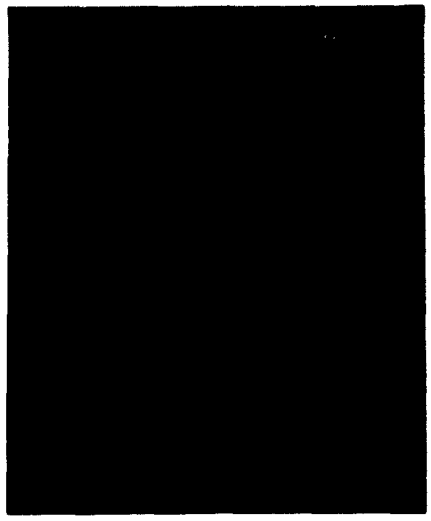

(a)

Time t - 0

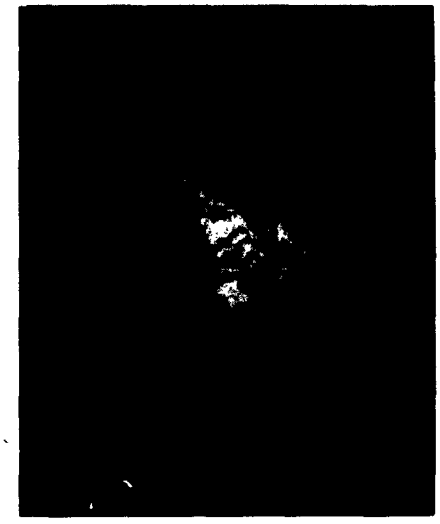

(b)

Time t = 2 minutes

(c)

Time t = 4 minutes

(d)

Time t = 5 minutes

Distribution List for Progress Reports
Generated Under NObsr-87478

	No. Copies
Chief, Bureau of Ships Department of the Navy Washington 25, D. C. Attn: Code 681A2C (H. Nordenberg)	4
Chief, Bureau of Ships Department of the Navy Washington 25, D. C. Attn: Code 335	3
Director Naval Research Laboratory Washington 25, D. C. Attn: Technical Library	1
Commander New York Naval Shipyard Material Laboratory Naval Base Brooklyn 1, New York Attn: Technical Library	1
Chief, Bureau of Naval Weapons Department of the Navy Washington 25, D. C. Attn: Code RAAV4123	1
Commanding Officer and Director U. S. Navy Electronics Laboratory San Diego 52, California Attn: Mr. R. B. Jordan	1
Director U. S. Navy Underwater Sound Laboratory New London, Connecticut Attn: Technical Library	1
Director Naval Ordnance Laboratory Corona, California Attn: Mr. Robert Conger	1
Commander Navy Ordnance Laboratory Silver Spring, Maryland Attn: Technical Library	1

	No. Copies
Senior Naval Liaison Officer U. S. Navy Electronics Liaison Office Bay 4D119 U. S. Army Signal Research and Development Laboratory Fort Monmouth, New Jersey	1
Office of Naval Research Washington 25, D. C. Attn: Code 421 (Dr. Sorrows)	1
Director National Bureau of Standards Washington 25, D. C. Attn: Mr. G. Shapiro	1
Commanding Officer Diamond Ordnance Fuze Laboratory Washington 25, D. C. Attn: Mr. P. Franklin	1
Director National Bureau of Standards Boulder Laboratories Boulder, Colorado Attn: Technical Library	1
Commander Armed Services Technical Information Agency Arlington Hall Station Arlington 12, Virginia	10
Advisory Group on Electron Devices 8th Floor 346 Broadway New York 13, New York	2
Commanding General U. S. Army Signal Research and Development Laboratory Fort Monmouth, New Jersey Attn: SIGRA/SL-PEP (Mr. H. L. Stout)	1
Commanding General U. S. Army Signal Supply Agency 225 South 18th Street Philadelphia 3, Pennsylvania	1
Commander Aeronautical Systems Division Wright-Patterson Air Force Base, Ohio Attn: Mr. Carl K. Greene (WWRNEM-1)	1

	No. Copies
Commander Rome Air Development Center, ESD Griffiss Air Force Base, New York Attn: RCSSP (Mr. P. Giannico)	1
Inspector of Naval Material Department of the Navy 1783 East 11th Street Cleveland 14, Ohio Attn: Mr. John P. Sturges	1
Inspector of Naval Material Department of the Navy 1783 East 11th Street Cleveland 14, Ohio Attn: Mr. J. Heinal	1